# CHAPTER IV

# RESULTS AND DISCUSSION

## 4.1 Surface Characterization by Specular Reflection Technique

Figure 4.1 showed infrared spectra of polymer and polymer composites (*i.e.*, polypropylene (PP), poly(styrene-co-acrylonitrile), hydroxyapatite/polypropylene (HA/PP)) acquired by the specular reflection technique.

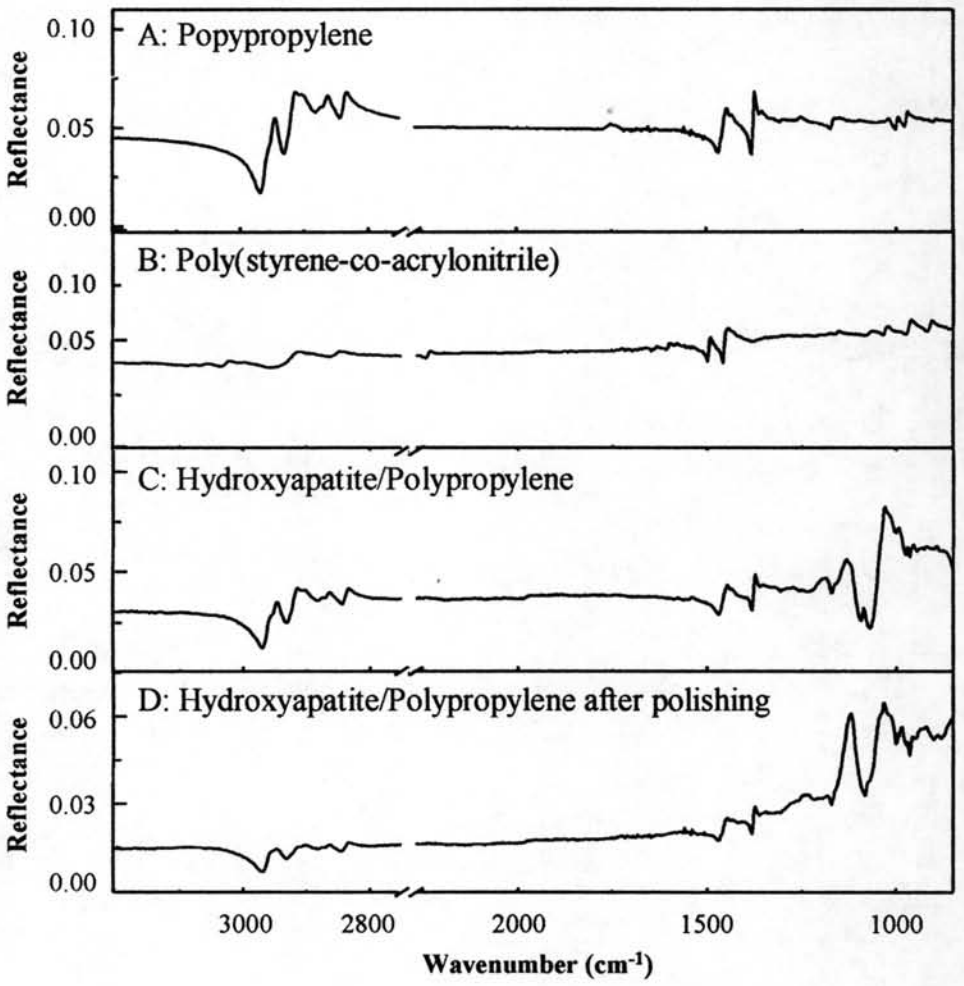


**Figure 4.1** Specular reflection spectra of (A) polypropylene, (B) poly(styrene-co-acrylonitrile), (C) hydroxyapatite/polypropylene composites before polishing, and (D) hydroxyapatite/polypropylene composites after polishing with a sand paper.

The observed spectra showed derivative-type peak shape in all characteristic absorptions which were not easily interpreted. A mathematic process known as Kramers-Kronig (KK) transformation can be employed for making a specular reflection spectrum become absorption-like spectrum. Figure 4.2 showed the KK-transformed spectra of the spectra shown in figure 4.1. The KK-transformed spectra of polypropylene and poly(styrene-co-acrylonitrile) were easily interpreted. However, they exhibited the derivative-type peak shape in some region. This observation indicated that there was diffuse reflectance or scattering radiation interfering with the specular reflectance radiation.

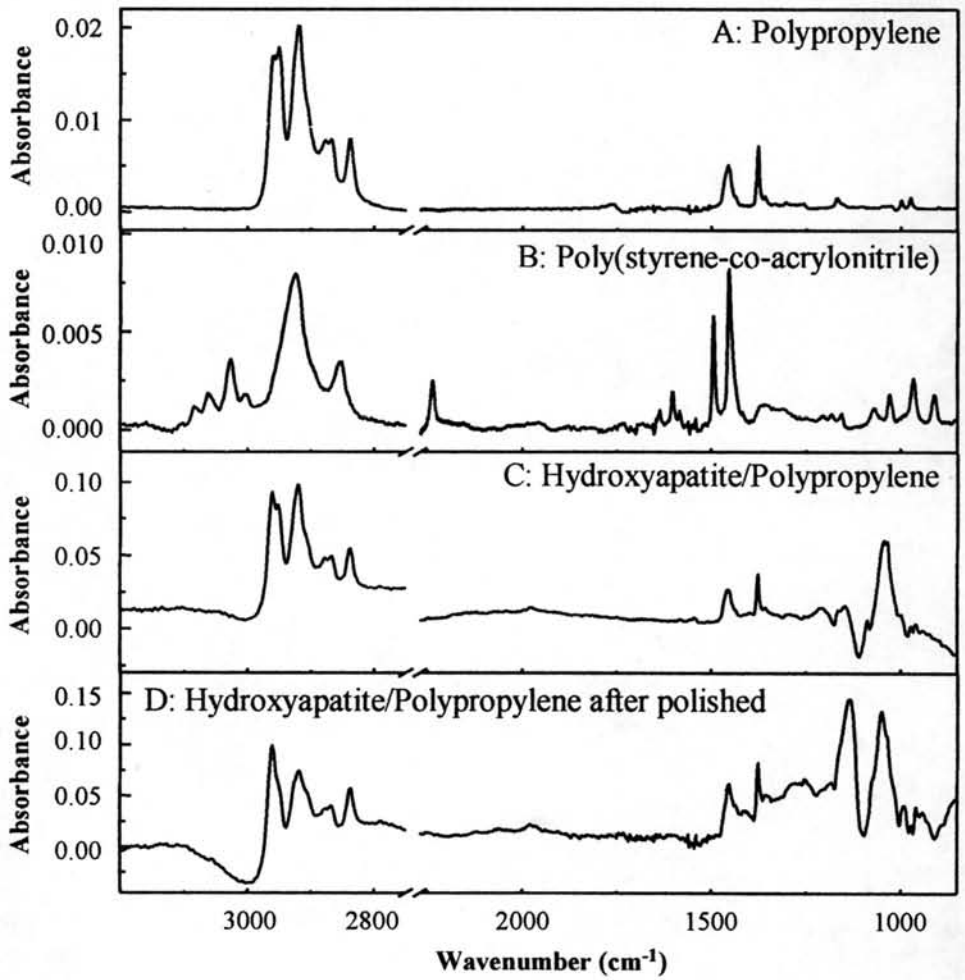


**Figure 4.2** KK-transformed spectra of specular reflection spectra shown in Figure 4.1. (A) polypropylene, (B) poly(styrene-co-acrylonitrile), (C) hydroxyapatite/polypropylene composites before polishing, (D) hydroxyapatite/polypropylene composites after polishing with sand paper.

In case of hydroxyapatite/polypropylene composites, the KK-transformed spectrum was not easily interpreted (Figure 4.2 (C)). Although the specimen was prepared by injection molding process, the surface of specimen is not smooth enough. The rough surfaces can be smoothed by polishing or cutting with a sharp razor blade. However, the polishing may also decrease the efficiency of the specular reflection or introduce diffuse reflection and scattering phenomenon (Figure 4.2 (D)). The KK-transformation works well only if the spectrum was purely specular reflection. As the results, the specular reflection technique was not appropriate for characterization of polymer and/or polymer composite with a rough surface such as hydroxyapatite/ polypropylene composites.

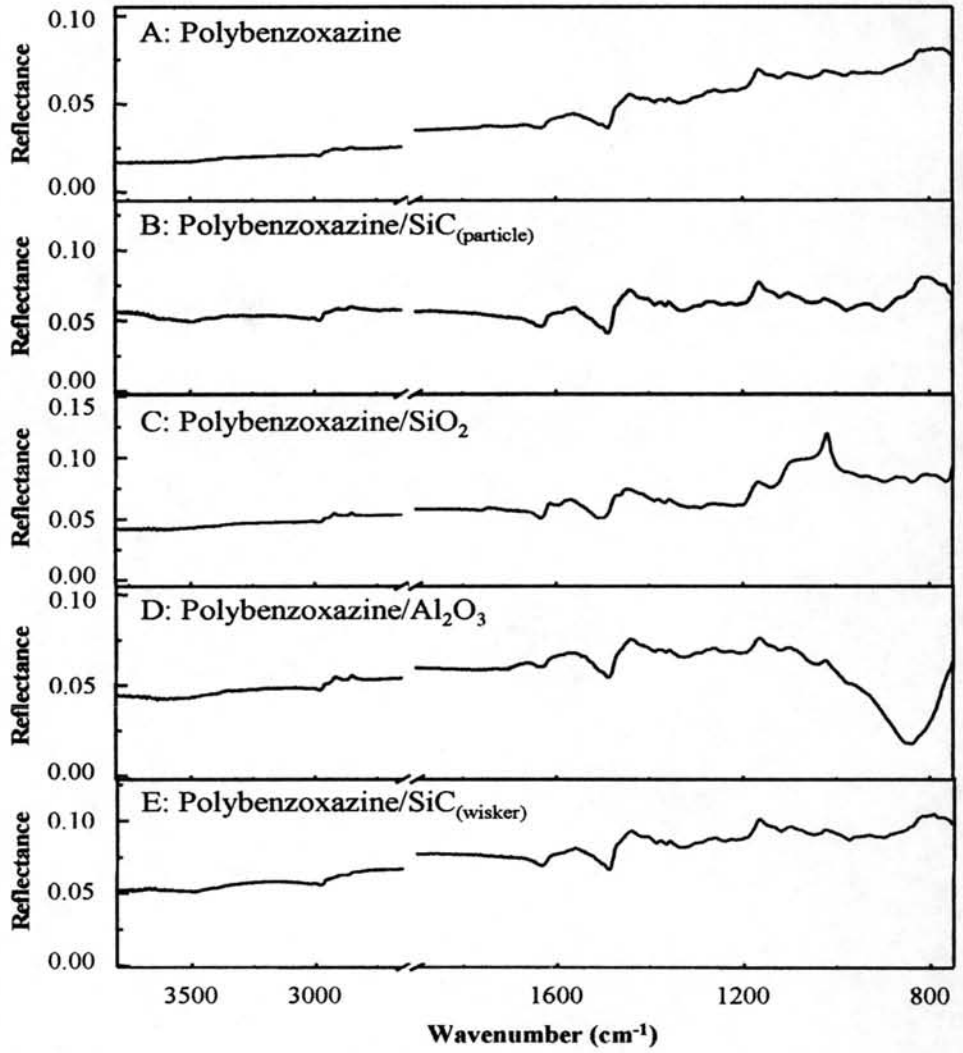


**Figure 4.3** Infrared spectra of (A) polybenzoxazine, (B) polybenzoxazine/ $SiC_{(particle)}$, (C) polybenzoxazine/$SiO_2$, (D) polybenzoxazine/$Al_2O_3$, and (E) polybenzoxazine/$SiC_{(wisker)}$ composites acquired by specular reflection technique.

For the homogeneity investigation of resin and its composites (*i.e.*, polybenzoxazine, polybenzoxazine/$Al_2O_3$, polybenzoxazine/$SiO_2$, polybenzoxazine /$SiC_{(particle)}$, polybenzoxazine/$SiC_{(wisker)}$) acquired via specular reflection, the specimens were prepared by compression molding techniques and there were no additional sample preparation. Figure 4.3 shows specular reflection spectra of the resin and its composites. The observed spectra showed derivative-type peak shape in all characteristic absorptions which are not easily interpreted.

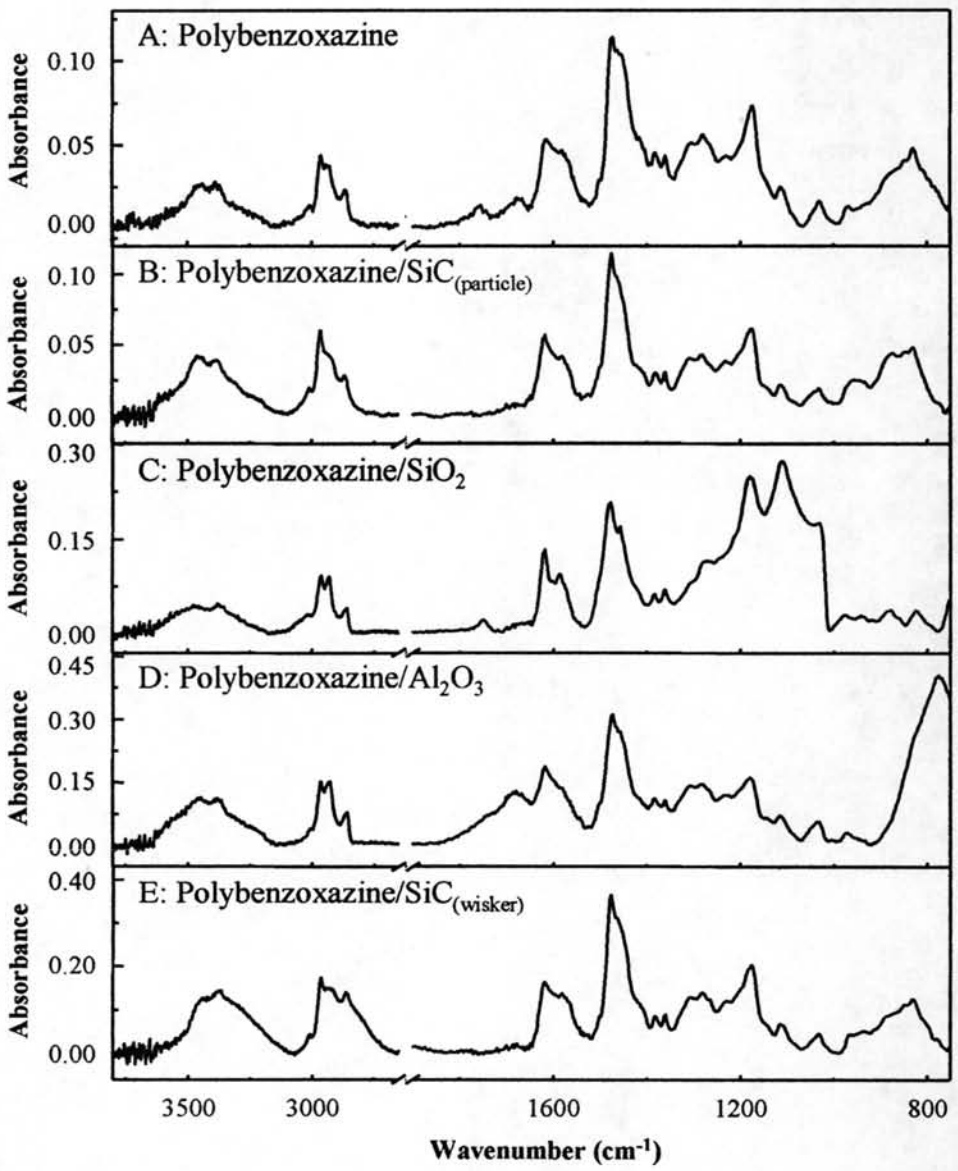


**Figure 4.4** KK-transformed spectra of specular reflection spectra shown in Figure 4.3. (A) polybenzoxazine, (B) polybenzoxazine/$SiC_{(particle)}$, (C) polybenzoxazine/$SiO_2$, (D) polybenzoxazine/$Al_2O_3$, and (E) polybenzoxazine/$SiC_{(wisker)}$ composites.

Figure 4.4 shows the KK-transformed spectrum of polybenzoxazine and its composite. The KK transformed spectra showed absorption type spectral features and were easily interpreted. Since the specimens had a smooth and glossy surface, pure reflection at the surface was achieved. This made the KK-transformed spectra become absorption-like spectra without any reflection-type peak shape interference. However, most of the polymer composite does not have a smooth and glossy surface. The KK-transformed spectra still had a reflection-type feature due to the scattering content in the original spectra (reflection spectra). Thus, the specular reflection technique may be not suitable for polymer composites or polymer with rough surface.

Due to un-reproducible smooth surfaces and reflection spectra, the specular reflection technique was not appropriate for homogeneity analysis of polymer composite. A novel approach such as ATR FT-IR microspectroscopy with a Ge μIRE and diamond μIRE were employed for the homogeneity analysis of polymer blends and composites.

## 4.2 Comparison of Spectra Acquired by Ge μIRE and Diamond μIRE

Figure 4.5 shows ATR FT-IR spectra of hydroxyapatite/polypropylene (HA/PP); polypropylene (PP) and poly(styrene-co-acrylonitrile) acquired by the Ge μIRE and diamond μIRE. The spectral features observed by the Ge μIRE were slightly different from those acquired by the diamond μIRE, especially the relatively absorbance. There are two main reasons for the differences. The first is the low refractive index of diamond ($n_{Dimond}$ = 2.417) compared to that of germanium ($n_{Ge}$=4.0).

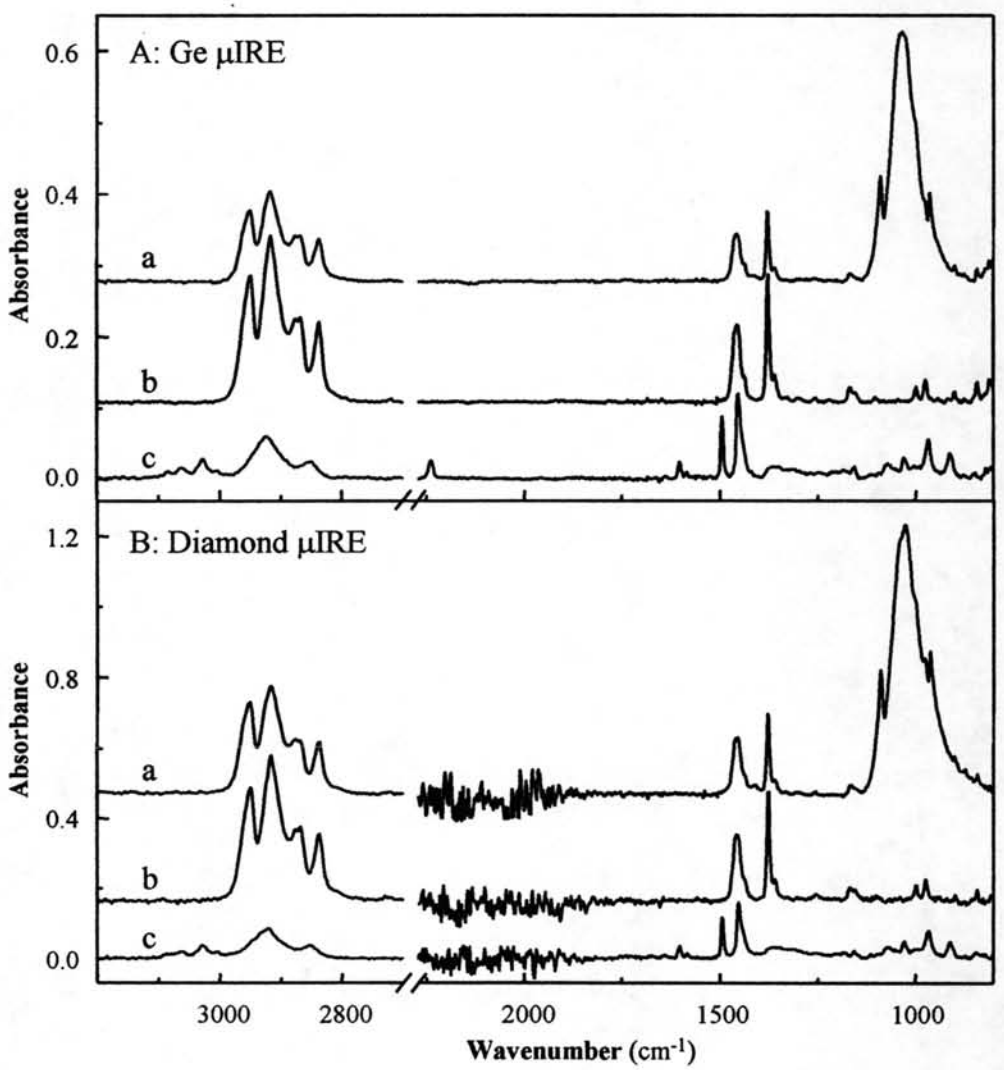


**Figure 4.5** ATR FT-IR spectra of (a) hydroxyapatite/polypropylene composites, (b) polypropylene, and (c) poly(styrene-co-acrylonitrile) measured by (A) Ge μIRE and (B) diamond μIRE.

Under the ATR condition, the absorption in absorbance unit of the material attached to the IRE can be expressed in terms of the experimental conditions and material characteristics by as follows:

$$A(\theta,\nu) = \frac{2\pi\nu}{\ln(10)\, n_{IRE} \cos\theta} n_{sample}(\nu)\, k_{sample}(\nu)\, d_p(\theta,\nu)\, \langle E_0^2(\theta,\nu)\rangle \qquad (1)$$

where θ is the angle of incidence, ν is the frequency of the incident radiation (*i.e.*, in wavenumber unit), $n_{Sample}$ and $k_{Sample}$, respectively, are the refractive index and the absorption index of the sample, $d_p(\theta,\nu)$ is the penetration depth, and $\langle E_0^2(\theta,\nu)\rangle$ is the mean square evanescent electric field (MSEvF) at the interface. The penetration depth is given in terms of experimental conditions and material characteristics by

$$d_p = \frac{\lambda}{2\pi n_{IRE} [\sin^2\theta - (n_{sample}(\nu) / n_{IRE})^2]^{1/2}} \qquad (2)$$

Equation 2 shows the association between the refractive index of IRE and the penetration depth. Due to the refractive index of diamond is lower than that of the Ge, the penetration depth is greater. As a result, the diamond IRE gave a higher absorption of material than Ge IRE.

The second reason is the good contact between the IRE and the specimens. Although Ge μIRE has a small contact area (100 μm in diameter), the contact between rough surface of polymer composite was not enough to achieve an optical contact (Figure 4.6). Since diamond is hardness known material, the employed diamond IRE with a the small culet (contact area 30 μm in diameter) made an unnoticeable dent on the surface of the specimen. As the surface of the polymer attained an optical contact with the pavilion facet of diamond, good ATR FT-IR spectra could be acquired.

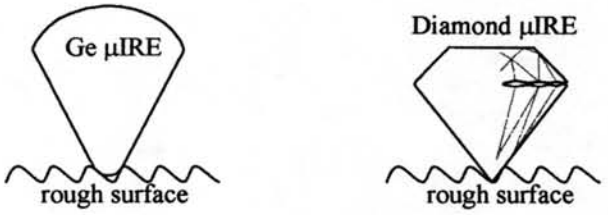


**Figure 4.6** Schematic illustration of the contact between IRE (Ge μIRE and diamond μIRE) and rough surface of specimen.

However, the ATR FT-IR spectra acquired from diamond μIRE showed a high noise level at 2400-1900 $cm^{-1}$ (Figure 4.5 (B)). This region is corresponding to an absorption band of diamond namely the two-phonon absorption. Since the two-phonon absorption is very strong, the observed ATR FT-IR spectrum of a specimen in the region was obscured by the absorption of the two phonon absorption. The high noise level was normally observed in the two-phonon region when the diamond IRE was employed as a reference for the spectral acquisition.

The three principle absorption bands of diamond includes, one-phonon at 1400-900 $cm^{-1}$, two-phonon at 2650-1500 $cm^{-1}$, and three-phonon at 3900-2650 $cm^{-1}$. They are associated with impurities and defects in the diamond crystal structure [35]. Although the two-phonon absorption always exhibits over absorption, it has little effect on the analytical applications since small number of functional group has absorption in this region. In case of poly(styrene-co-acrylonitrile), the absorption band of cyano group (CN) at 2230 $cm^{-1}$ was obscured by the two phonon absorption of diamond absorption band at the two phonon region (Figure 4.5 B (c)).

## 4.3 Homogeneity Investigation of Polymer by ATR FT-IR Technique

The homogeneity investigations of polymer and composites were divided into two parts: the surface mapping and depth profiling analysis. For the surface mapping, the area map was performed. To construct a surface map, a sampling area of the map was selected through the built-in infrared objective. The spectral point-by-point mapping was done in a grid pattern with the computer x-y axis controlling microscope stage. For depth profiling characterization, the line map was employed. The specimen was cut with an oblique angle in order to increase the distance along the cross-section surface. The line map was drawn across the cross-section surface. ATR FT-IR spectra along the grid were employed for construction of the chemical image of chemical species on the surface. Variation of absorption band unique to a chemical species indicated the change of the concentration across the measured area. As the results, the homogeneity or uniformity of a composite can be determined from the chemical image constructed from an absorption band as unique to the polymer matrix or that of the filler. To construct the surface-map and line-map, Ge μIRE and diamond μIRE were employed. By making a good contact between the IRE and the surface, ATR FT-IR spectra of the contacted surface can be acquired.

### 4.3.1 Polypropylene

The polymer surface approximately 1 × 2 mm. was mapped. The uses of step-size of 200 μm, resulting in data sets of 50 spectra were achieved. ATR FT-IR spectra of polypropylene at various positions along the surface acquired by Ge μIRE and diamond μIRE were shown in Figure 4.7 (A) and Figure 4.7 (B), respectively. The peak assignments of ATR FT-IR spectrum of polypropylene are shown in Table 4.1. As seen in the figures, all ATR FT-IR spectra show the same spectral feature. The same spectral feature reveals that the sample is the same chemical components at various positions of the area map.

The superimpositions of polypropylene spectra were observed and shown in Figure 4.8 (A1) and Figure 4.8 (B1). The distribution of functional group with the absorption at 2917 $cm^{-1}$ on the surface of area map can be seen in Figure 4.8 (A2),

and Figure 4.8 (B2). The image was produced by displaying or plotting the infrared band intensity in the recorded spectra as a function of the sample x-y coordinates.

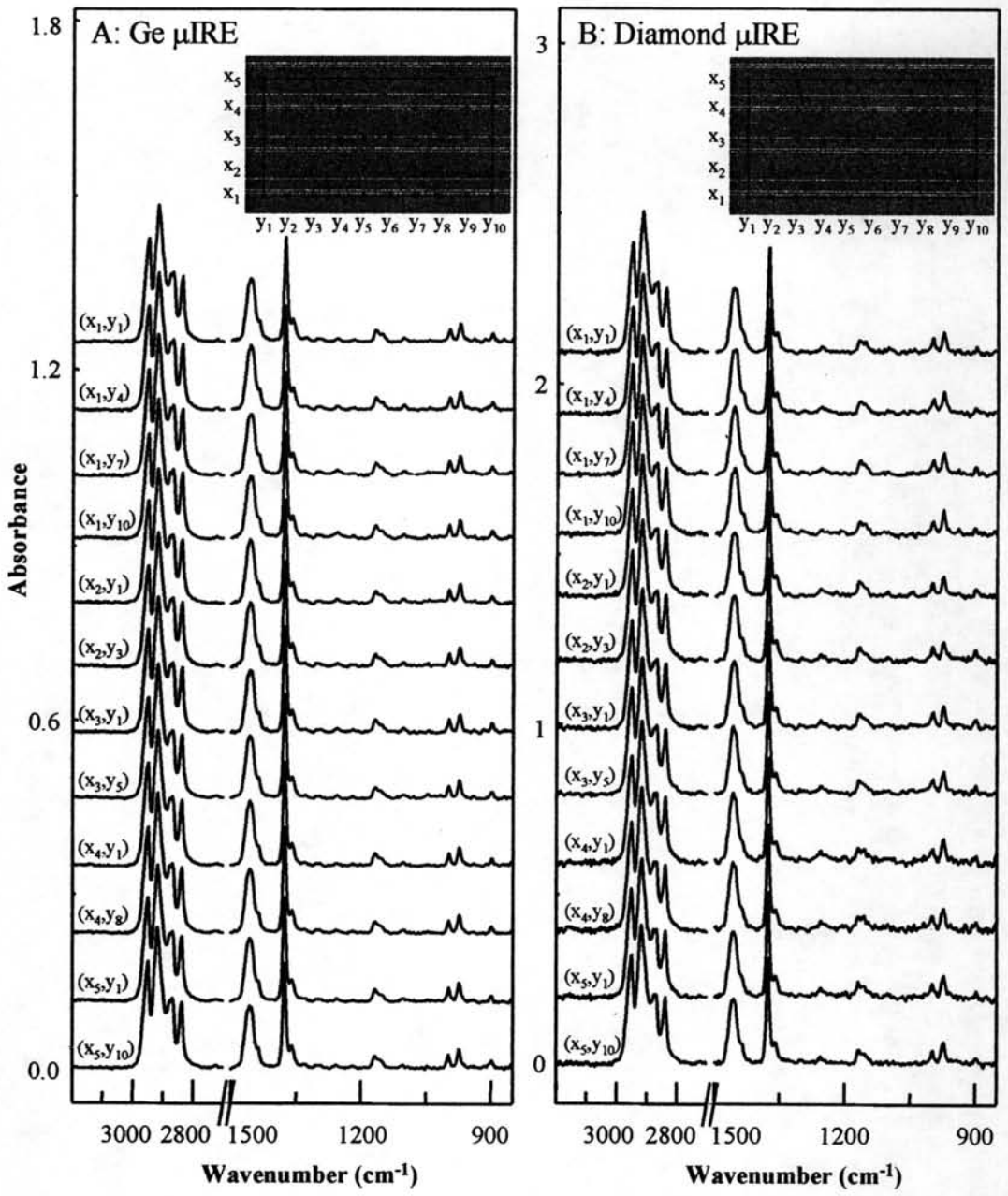


**Figure 4.7** ATR FT-IR spectra at selected position on the surface of polypropylene specimen measured by (A) Ge μIRE and (B) diamond μIRE.

The color on contour map (2D) referring to the absorption of each spectrum was used to estimate the variation of absorption of the polypropylene. The absorbance is in the range of 0.250-0.245 for Ge μIRE and 0.415-0.445 absorbance unit for diamond μIRE. The obtained spectra revealed small variation of the absorbance, this variation was comparable to the noise level. The noise level (peak-to-peak noise) of the observed spectra was 0.01 for Ge μIRE and 0.02 absorbance unit for diamond μIRE. The observed phenomena indicated that ATR surface mapping of a homogeneous polymer or homogeneous composite had the variation of absorption comparable to the noise level.

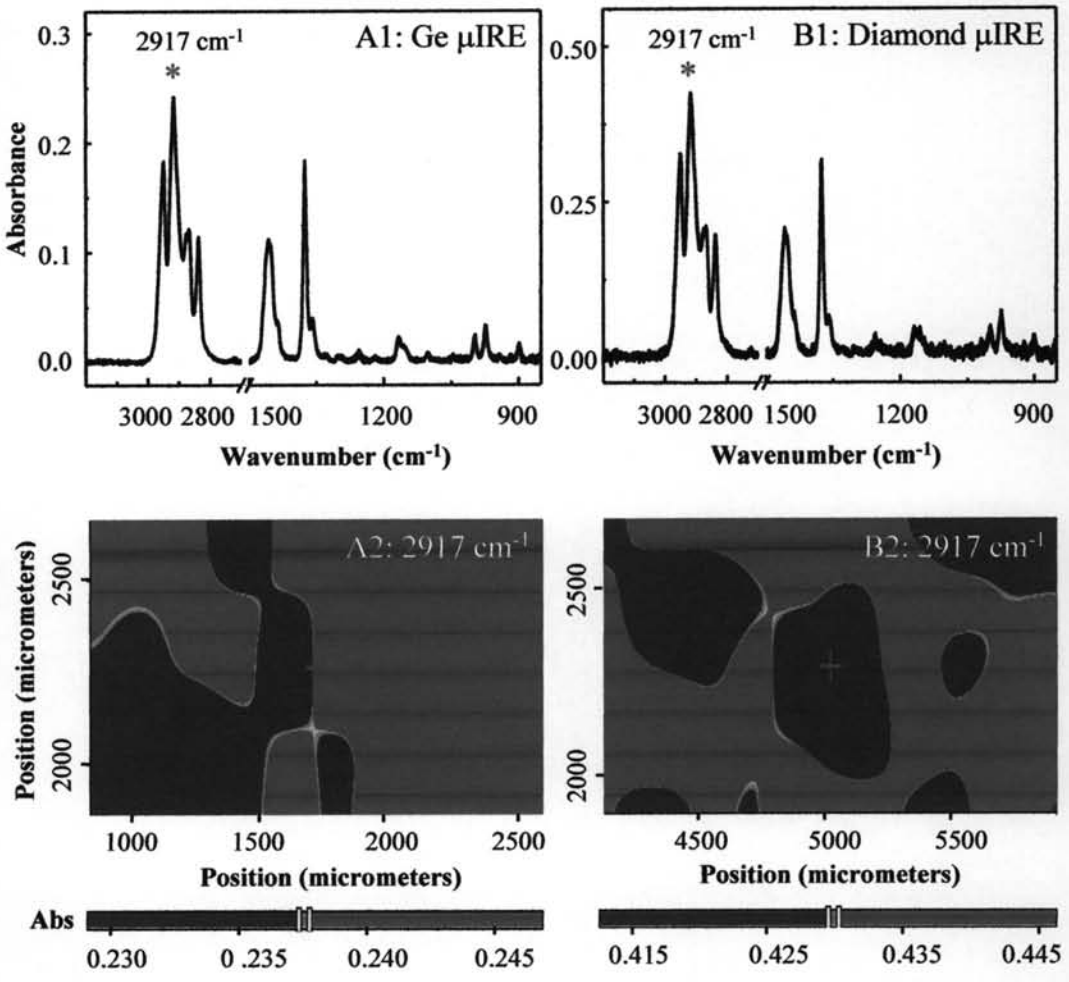


**Figure 4.8** Superimposition of ATR FT-IR spectra of polypropylene at various positions shown in Figure 4.7 were acquired by (A1) Ge μIRE and (B1) diamond μIRE. Figure 4.8 (A2) and Figure 4.8 (B2) were the contour map of the polypropylene with the absorption at 2917 $cm^{-1}$ as the profile mapping.

**Table 4.1** Infrared peak assignments of polypropylene [39].

| Peak Position ($cm^{-1}$) | Assignments |
|---|---|
| 2948 | Asymmetric C-H stretching of $CH_3$ |
| 2917 | Asymmetric C-H stretching of $CH_2$ |
| 2876 | Symmetric C-H stretching of $CH_3$ |
| 2838 | Symmetric C-H stretching of $CH_2$ |
| 1456 | C-H bending of $CH_3$ |
| 1436 | C-H bending of $CH_2$ |
| 1375 | C-H bending of $CH_3$ |
| 1359 | C-H bending of $CH_2$ |
| 1166 | C-C stretching |
| 997, 973 | C-H rocking of $CH_3$ |
| 824 | C-H bending of CH |

The depth dependence study of homogeneous polypropylene was investigated by line mapping along the cross-section surface. Figure 4.9 (A) and Figure 4.9 (B) show ATR FT-IR spectra of polypropylene collected by the Ge μIRE and diamond μIRE, respectively. As seen in the figures, all ATR FT-IR spectra show the same spectral feature. The spectral feature shows that the sample was the same chemical components at various positions at area map.

The superimpositions of polypropylene spectra from both IREs were shown in Figure 4.10 (A1) and Figure 4.10 (B1). To make sure that the absorption magnitudes of spectra are the same, the 3D color codes were shown in Figure 4.10 (A2) and Figure 4.10 (B2), respectively. The absorbance in the CH-stretching is in the range of 0.19-0.21 for Ge μIRE and 0.23-0.25 absorbance unit for diamond μIRE. Although the observed spectra revealed small variation of the absorbance, this variation was comparable to the noise level. The noise level (peak-to-peak noise) of the observed spectra was 0.01 for Ge μIRE and 0.02 absorbance unit for diamond μIRE. The observed phenomena indicated that ATR FT-IR spectra at various position of a homogeneous polymer were superimposed for all positions.

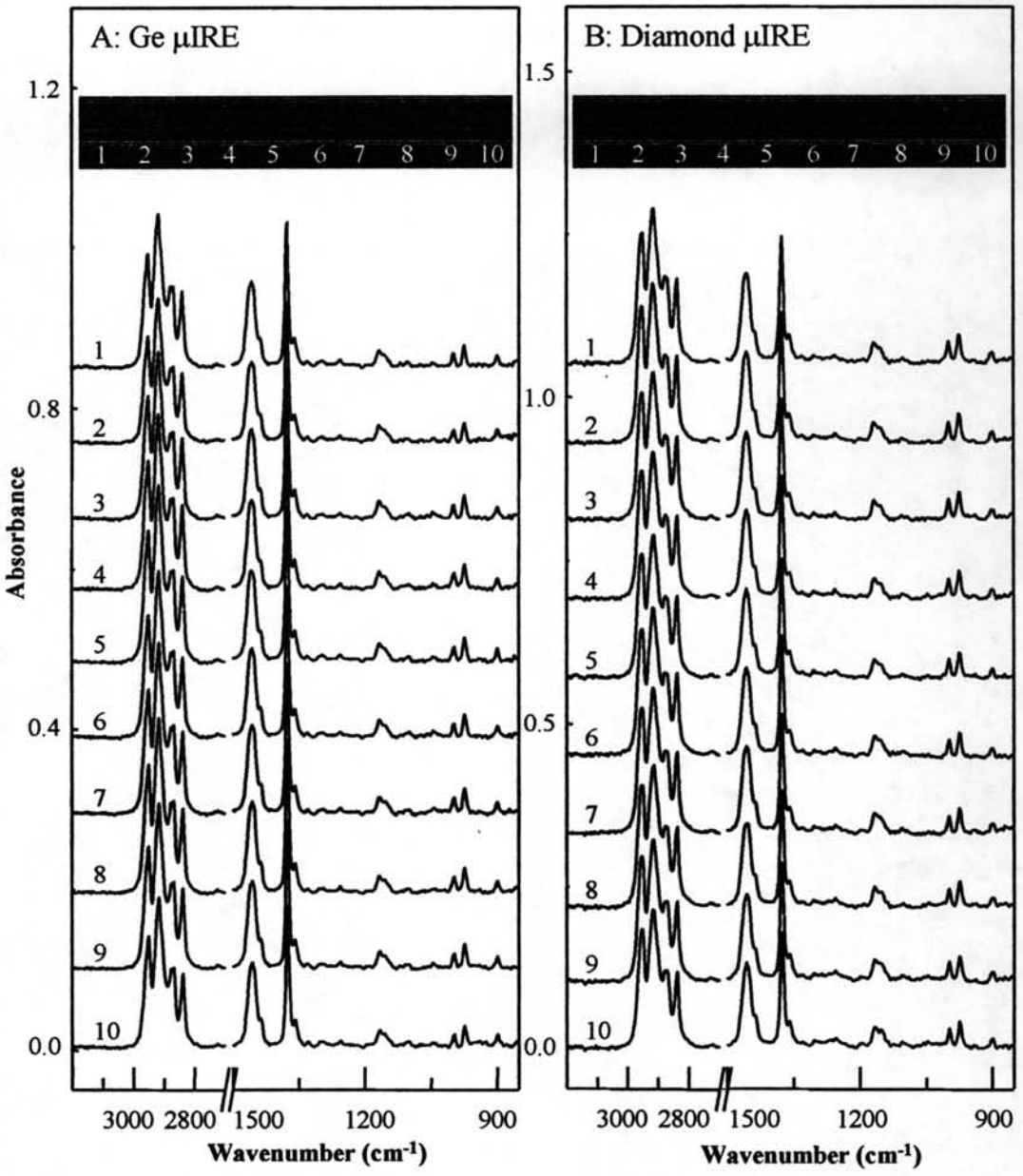


**Figure 4.9** ATR FT-IR spectra at selected position on the cross-sectioned surface of polypropylene specimen measured by (A) Ge μIRE and (B) diamond μIRE.

Since the infrared absorption band is unique to the chemical constituent and the absorption magnitude is directly related to concentration of sample, the same chemical constitution and the same absorption magnitude of spectra of an identical sample in ATR spectra acquired from both IREs reveal that polypropylene is the homogeneous sample.

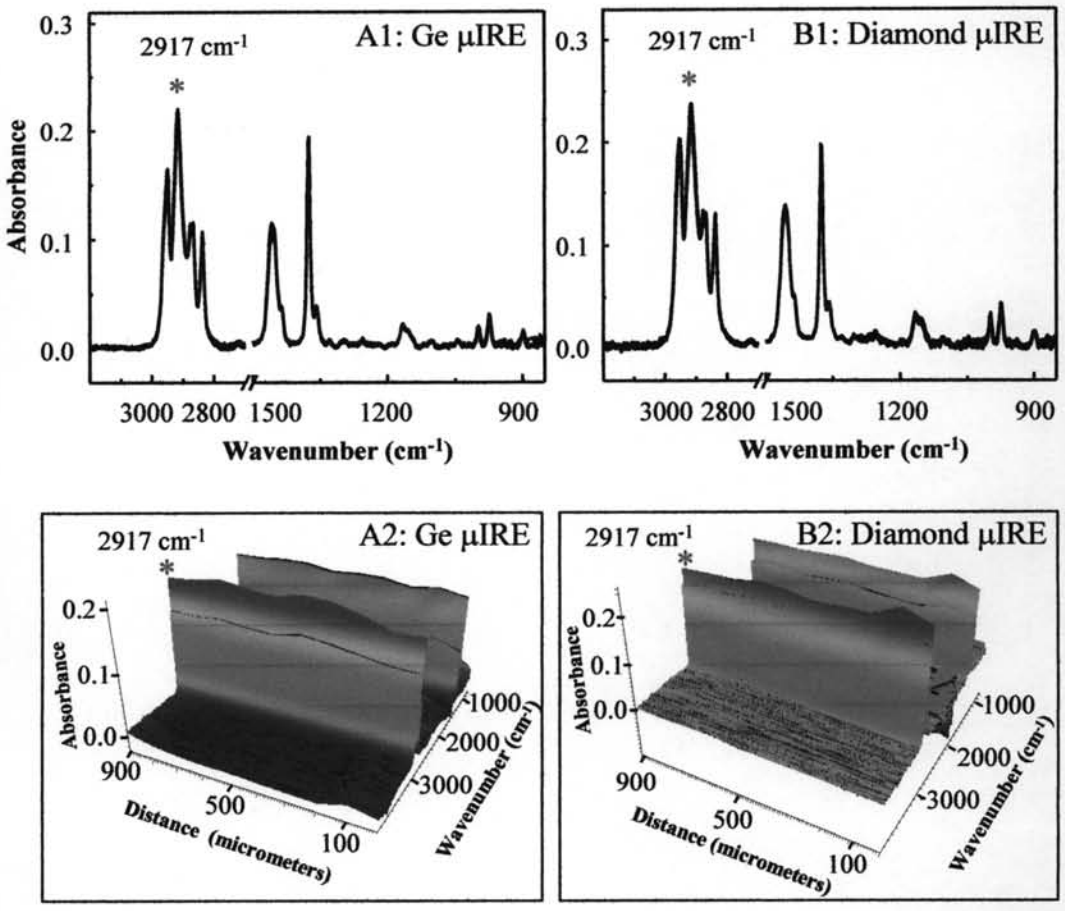


**Figure 4.10** Superimposition of ATR FT-IR spectra of polypropylene at various positions shown in Figure 4.9. Figure 4.10 (A2) and Figure 4.10 (B2) were 3D-image of the absorption band of the polypropylene.

### 4.3.2 Poly(styrene-co-acrylonitrile)

The surface of poly(styrene-co-acrylonitrile) approximately 1×2 mm was mapped. The step-size of 200 μm resulting in data sets of 50 spectra were collected. ATR FT-IR spectra of poly(styrene-co-acrylonitrile) at various grid position along the surface acquired by Ge μIRE and diamond μIRE were shown in Figure 4.11 (A) and Figure 4.11 (B), respectively. The peak assignments of ATR FT-IR spectrum of poly(styrene-co-acrylonitrile) are shown in Table 4.2. As seen in the figure, all ATR FT-IR spectra show the same spectral feature.

The superimpositions of poly(styrene-co-acrylonitrile) spectra were observed and were shown in Figure 4.12 (A1) and Figure 4.12 (B1). The same spectral features show that the sample was the same chemical components at various positions of the area map. They are superimposed at all positions.

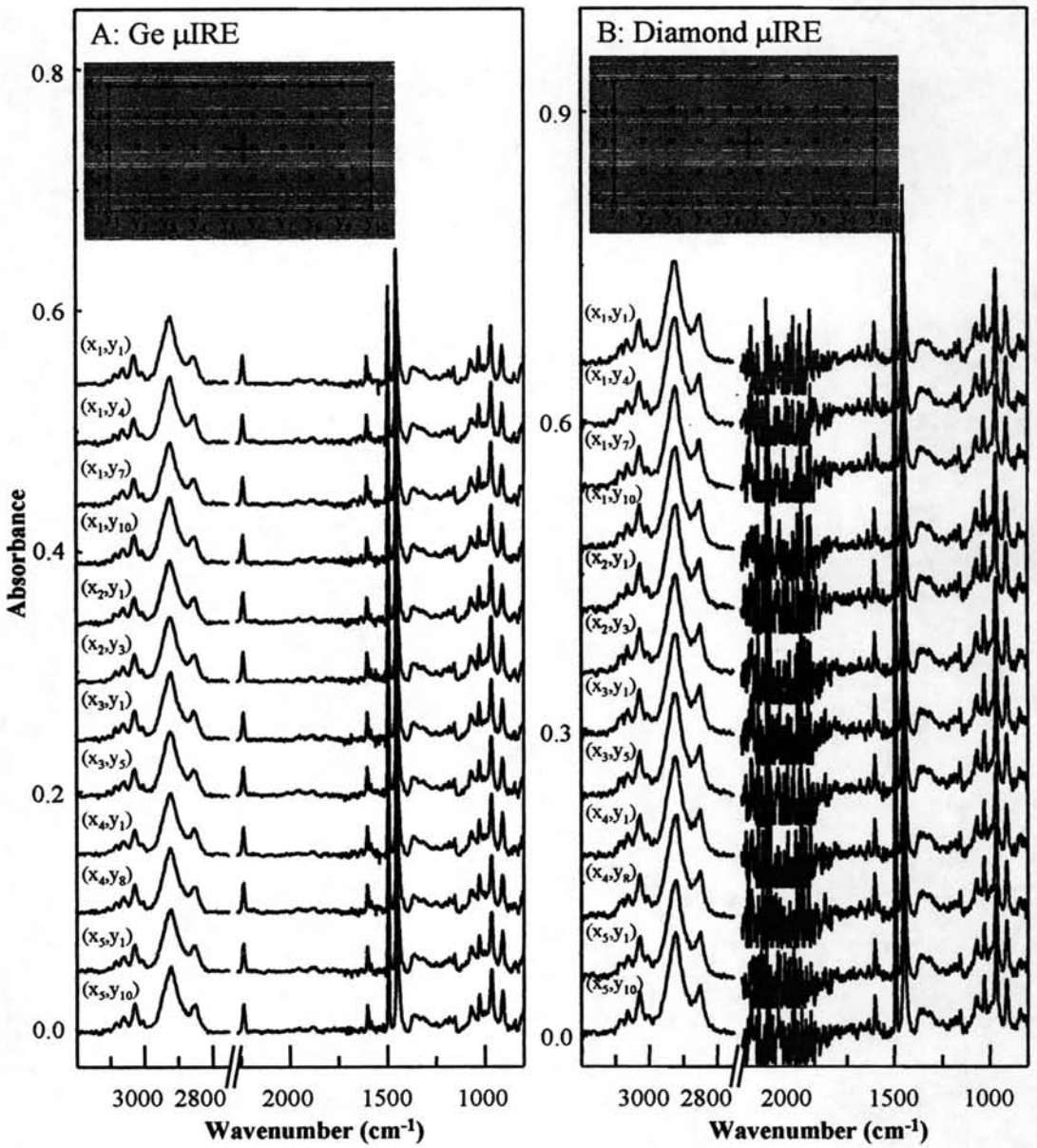


**Figure 4.11** ATR FT-IR spectra at selected position on the surface of poly(styrene-co-acrylonitrile) specimen measured by (A) Ge μIRE and (B) diamond μIRE.

Figure 4.12 (A2), and Figure 4.12 (B2) show the ATR FT-IR surface mapping of the poly(styrene-co-acrylonitrile) with the peak height at 2921 $cm^{-1}$ as the profile mapping. The color on the contour map referring to the absorption of each spectrum was used to estimate the variation of absorption of the poly(styrene-co-acrylonitrile). The absorbance of the CH-stretching absorption is in the range of 0.065-0.075 absorbance unit for Ge μIRE and 0.09-0.11 diamond μIRE.

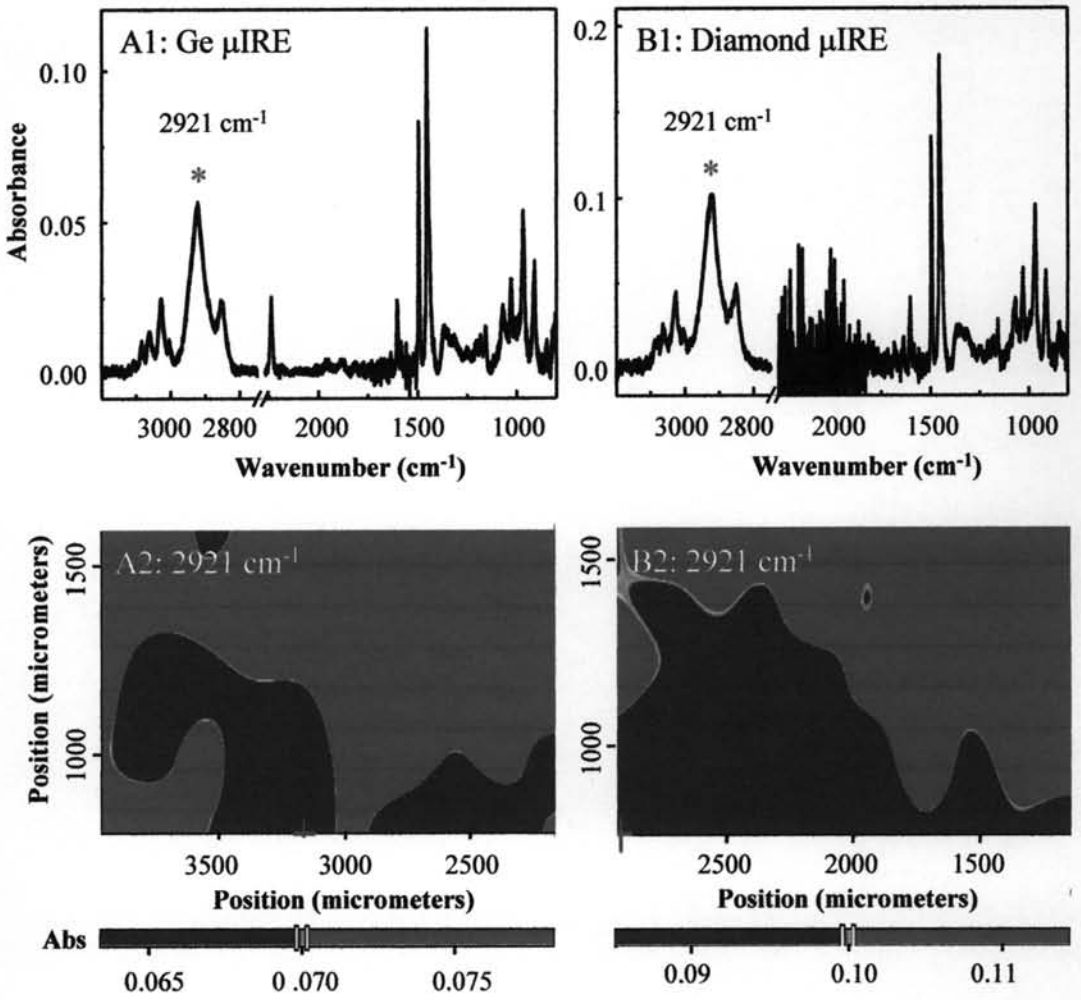


**Figure 4.12** Superimposition of ATR FT-IR spectra of poly(styrene-co-acrylonitrile) at various positions shown in Figure 4.11 acquired by (A1) Ge μIRE and (B1) diamond μIRE. Figures 4.12 (A2) and 4.12 (B2) were the contour map of the poly(styrene-co-acrylonitrile) with the absorption at 2921 $cm^{-1}$ as the profile mapping.

Although the obtained spectra reveal small variation of the absorbance, this variation is comparable to the noise level. The noise level (peak-to-peak noise) of the observed spectra was 0.01 for Ge μIRE and 0.02 absorbance unit for diamond μIRE. The observed phenomena indicated that ATR FT-IR spectra of a homogeneous polymer were superimposed for all positions.

**Table 4.2** Infrared peak assignments of poly(styrene-co-acrylonitrile) [39].

| Peak Position ($cm^{-1}$) | Assignments |
|---|---|
| 3081, 3055, 3027, 3001 | C-H stretching of aromatic |
| 2921 | Asymmetric C-H stretching of $CH_2$ |
| 2846 | Symmetric C-H stretching of $CH_2$ |
| 2238 | C≡N stretching |
| 1602, 1583, 1494, 1452 | C=C stretching of aromatic |
| 1452 | C-H bending of $CH_2$ |
| 1352 | C-H bending of $CH_2$ |
| 1184, 1156, 1070, 1029 | C-H in plane deformation of aromatic |
| 845, 759 | C-H out of plane deformation of aromatic |

The depth dependence study of the homogeneous poly(styrene-co-acrylonitrile) specimen was investigated by line mapping of cross-section surface. Figure 4.13 (A) and Figure 4.13 (B) show ATR FT-IR spectra of poly(styrene-co-acrylonitrile) observed by the Ge μIRE and diamond μIRE, respectively. The superimpositions of poly(styrene-co-acrylonitrile) spectra were achieved from both IREs and were shown in Figure 4.14 (A1) and Figure 4.14 (B1). To make sure that the absorption magnitudes of spectra are the same, the 3D color map were shown in Figure 4.14 (A2) and Figure 4.14 (B2), respectively. As seen in Figure 4.14 (A2), there was the absorption band of carbon dioxide ($CO_2$) in atmosphere at 2361 $cm^{-1}$ since the drawback of the system is $CO_2$ in atmosphere cannot be controlled. However, the absorption of $CO_2$ has no effect on the spectral analysis. Although the obtained spectra reveal small variation of the absorbance, this variation is comparable to the noise level. The noise level (peak-to-peak noise) of the observed spectra was

0.01 for Ge μIRE and 0.02 absorbance unit for diamond μIRE. The observed phenomena indicated that ATR FT-IR spectra of a homogeneous polymer were superimposed for all positions.

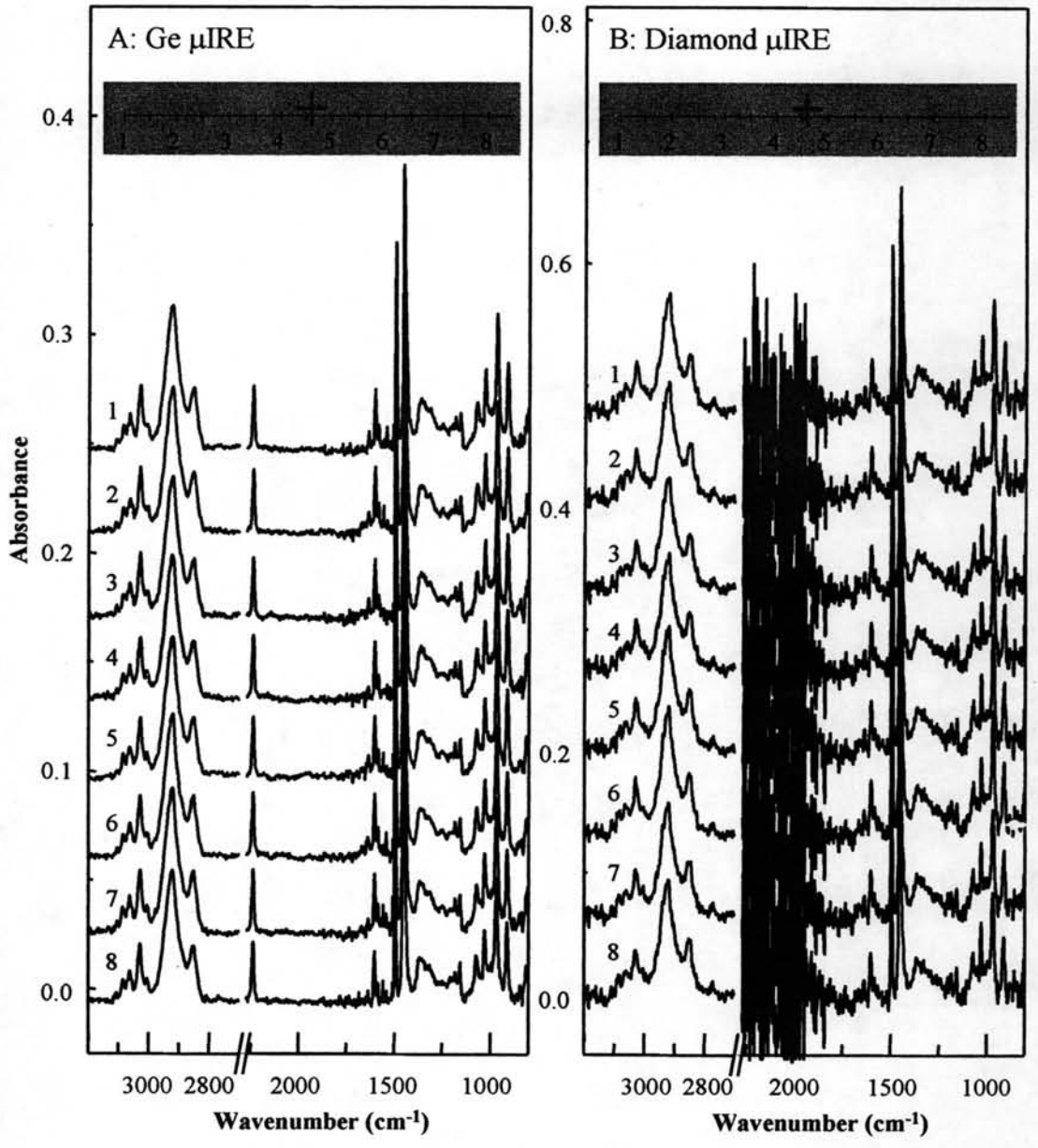


**Figure 4.13** ATR FT-IR spectra at selected position on the cross-section surface of poly(styrene-co-acrylonitrile) specimen measured by (A) Ge μIRE and (B) diamond μIRE.

Since the unique infrared absorption band is related to the chemical composition of sample and the absorption magnitude is directly related to concentration of sample, the same chemical information of spectra and the same absorption magnitude and identical sample in ATR spectra acquired from both IREs reveal that poly(styrene-co-acrylonitrile) is the homogeneous sample.

As the results in this section, it is concluded that ATR FT-IR microspectroscopy by using diamond and Ge as an IRE is the powerful tool to map the morphology of the distribution of component in polymer surface.

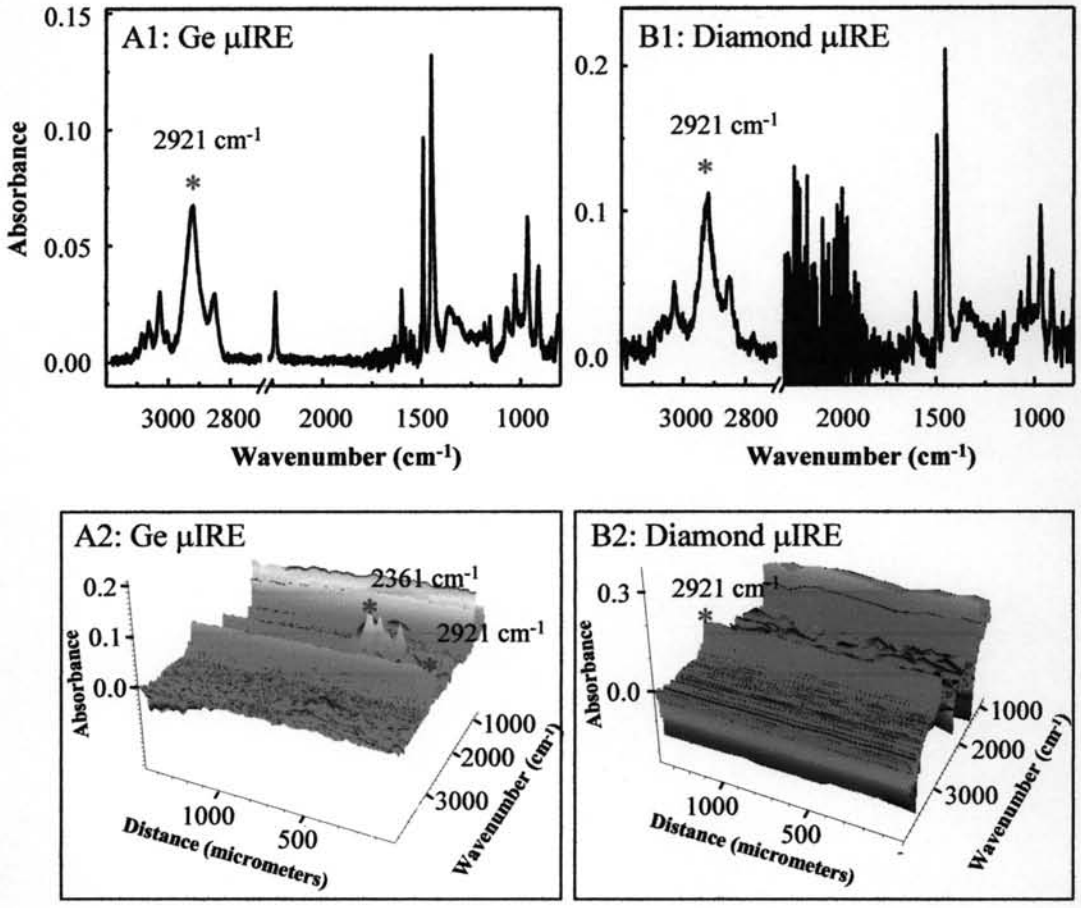


**Figure 4.14** Superimposition of ATR FT-IR spectra of poly(styrene-co-acrylonitrile) at various positions shown in Figure 4.13 acquired by (A1) Ge μIRE and (B1) diamond μIRE. Figure 4.14 (A2) and Figure 4.14 (B2) were 3D map of the poly(styrene-co-acrylonitrile).

## 4.4 Homogeneity Investigation of Polymer Composites by ATR FT-IR Technique

### 4.4.1 Hydroxyapatite/Polypropylene Composite

The analysis of hydroxyapatite/polypropylene composite, the specimen was prepared via mixing of 60% hydroxyapatite and polypropylene with internal mixing instument and injection molding technique. ATR FT-IR spectra of hydroxyapatite/ polypropylene composite at various positions acquired by Ge μIRE and diamond μIRE were shown in Figure 4.15. The peak assignments of ATR FT-IR spectrum of composite is shown in Table 4.3. For each IREs, the same absorption bands of spectral at various positions on the map were observed. The same absorption bands show that the chemical components were the same at various positions.

The superimpositions of hydroxyapatite/polypropylene composite spectra were obtained and shown in Figure 4.16. As seen in the figure, it was found that the intensity of each component in area map was different. Thus, it is clear that, the differences of peak shape at hydroxyapatite region were influenced from the difference of concentration.

Figure 4.16 (A2), and Figure 4.16 (B2) show the surface mapping of the hydroxyapatite/polypropylene composite with the peak height at 2917 $cm^{-1}$ and 1030 $cm^{-1}$ (*i.e.*, unique absorption of polypropylene and hydroxylapatite, respectively) as the profile mapping. The color code on contour map referring to the absorption of each spectrum was used to estimate the variation concentration of hydroxyapatite/ polypropylene composition across the surface. The observed map revealed large variation of the absorbance. The large variation of the unique absorption bands 0.05-0.20 for Ge μIRE and 0.19-0.35 absorbance units for diamond μIRE of polypropylene was greater than that of the noise level. The noise level (peak-to-peak noise) of the observed spectra was 0.02 for Ge μIRE and 0.02 absorbance unit for diamond μIRE. It is indicated that, the variation of absorption intensity of each absorption band is influent from the non-homogeneous distribution of each component.

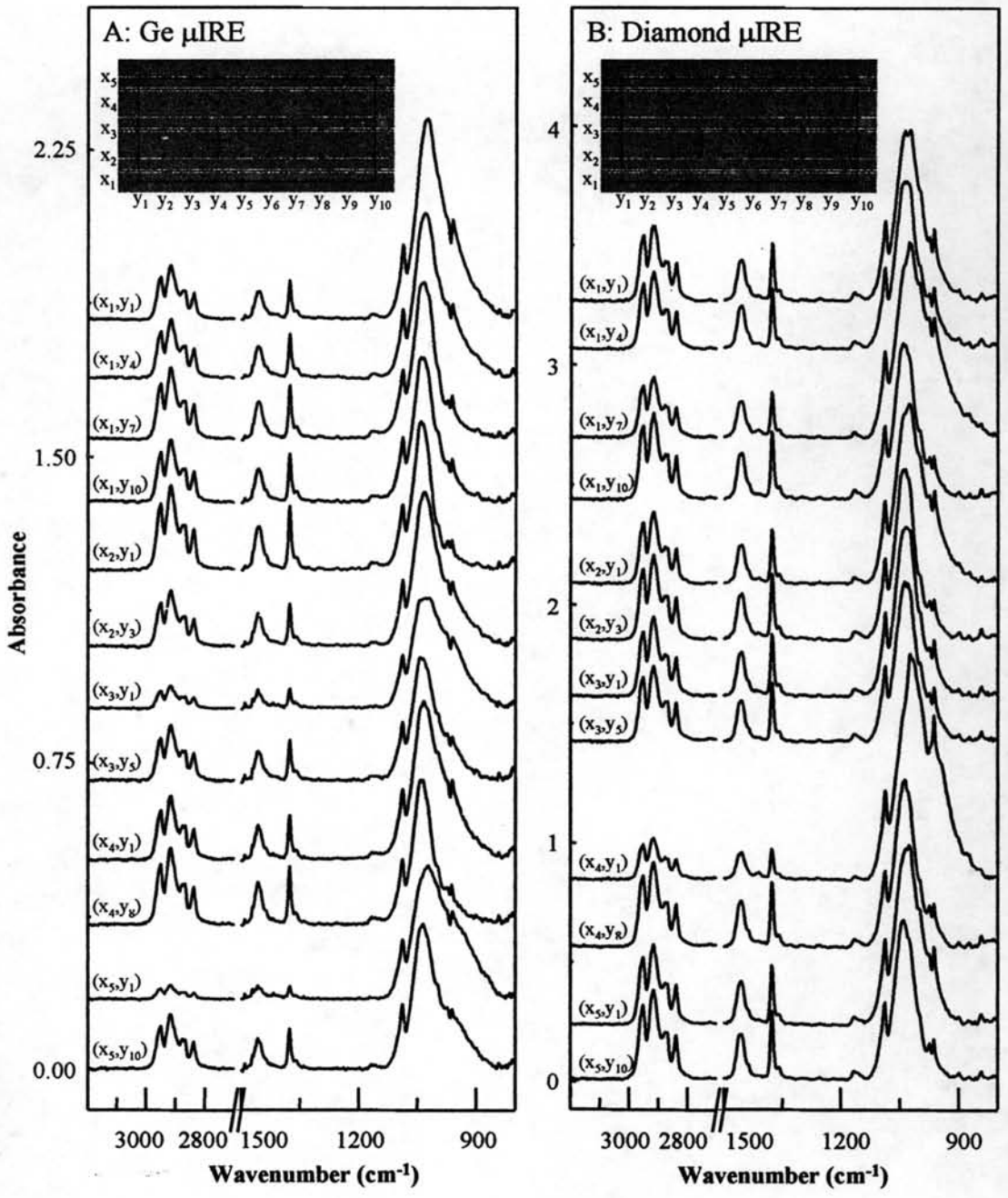


**Figure 4.15** ATR FT-IR spectra at selected position on the surface of hydroxyapatite/polypropylene specimen composite measured by (A) Ge μIRE and (B) diamond μIRE.

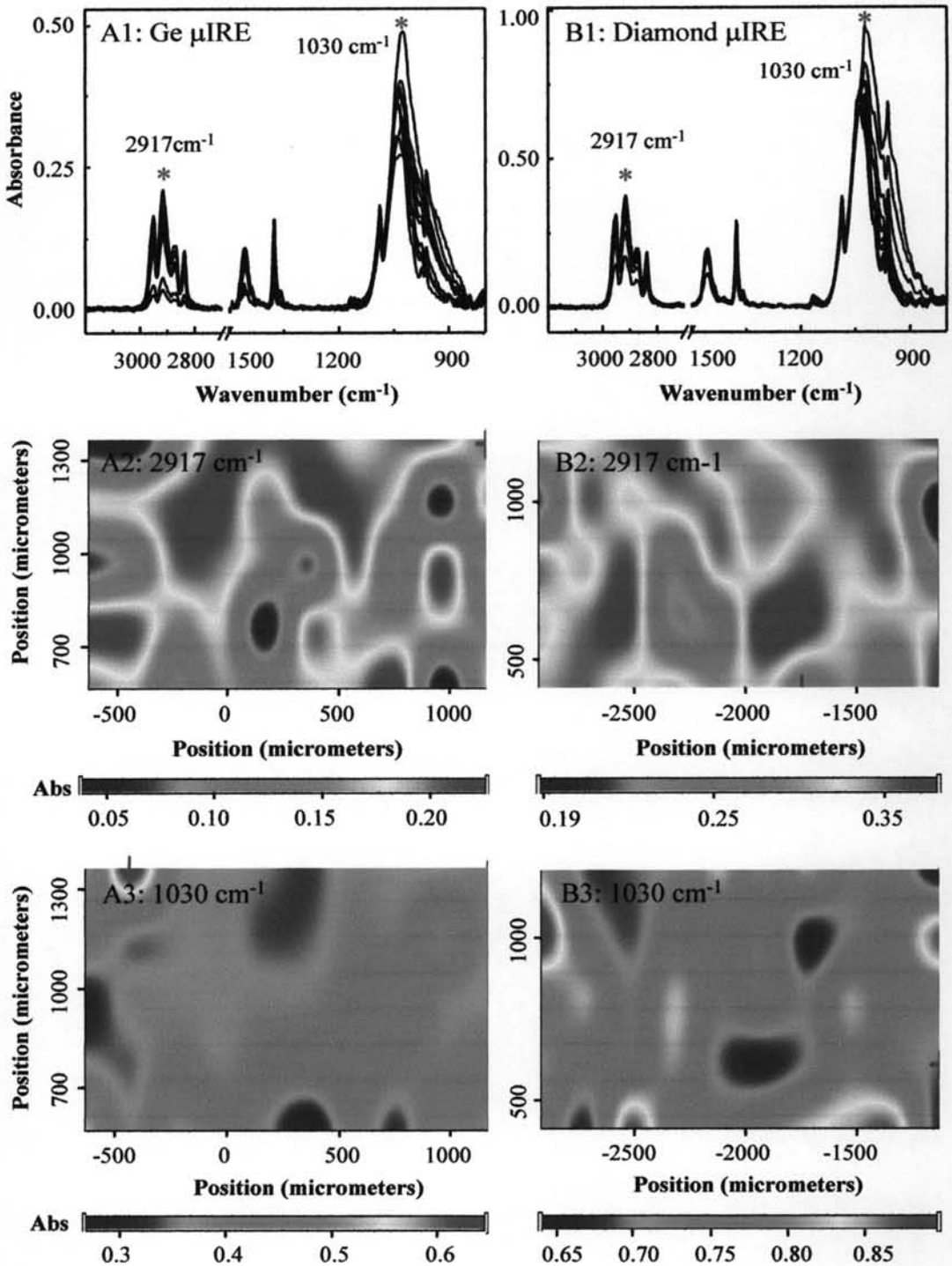


**Figure 4.16** ATR spectra and surface mapping of hydroxyapatite/polypropylene composite acquired by (A) Ge μIRE and (B) diamond μIRE. A1 and B1 were ATR spectra of the specimens at various positions. A2, B2 and A3, B3 respectively, showed the contour map of the composites with the peak height at 2917 $cm^{-1}$ and 1030 $cm^{-1}$ as the profile mapping.

As seen in Figure 4.16 (A2), the red regions in these images correspond to the high concentration of polypropylene. Thus in the same position on photographs in Figure 4.16 (A3) show the blue regions. That means, at the same position on the map if the band of hydroxyapatite is high concentration, it is low in concentration of polypropylene. For the analysis by using slide-on diamond μIRE (Figure 4.16 (B2) and (B3)), the results show in the same trend as that observed by the slide-on Ge μIRE.

The observed phenomena suggested that ATR FT-IR spectra at various positions of non-homogeneous polymer composites were not superimposed while the surface chemical map showed large variation in absorbance.

**Table 4.3** Infrared peak assignments of hydroxyapatite/polypropylene composite [39].

| Peak Position ($cm^{-1}$) | Assignments |
|---|---|
| 2948 | Asymmetric C-H stretching of $CH_3$ |
| 2917 | Symmetric C-H stretching of $CH_3$ |
| 2876 | Asymmetric C-H stretching of $CH_2$ |
| 2838 | Symmetric C-H stretching of $CH_2$ |
| 1456 | C-H bending of $CH_3$ |
| 1436 | C-H bending of $CH_2$ |
| 1411 | Asymmetric stretching of $CO_3^{2-}$ |
| 1375 | C-H bending of $CH_3$ |
| 1359 | C-H bending of $CH_2$ |
| 1166 | C-C stretching |
| 1086, 1030, 1021 | Asymmetric P-O stretching of $PO_4^{3-}$ |
| 997 | C-H rocking of $CH_3$ |
| 973 | C-H rocking of $CH_3$ |
| 960 | Symmetric P-O stretching of $PO_4^{3-}$ |
| 880, 873 | C-O stretching of $CO_3^{2-}$ |
| 842 | C-H bending of CH |

The depth dependence study of hydroxyapatite/polypropylene composite specimen was investigated by line mapping of cross-section surface. Figure 4.17 show ATR FT-IR spectra of hydroxyapatite/polypropylene composite observed by the Ge μIRE and diamond μIRE. For each IREs, the same absorption features at various positions on the map were observed. The same absorption band shows that the sample is the same chemical components at various positions at area map. However, the spectra at region of absorption band of hydroxyapatite show the difference of the peak absorption.

The superimpositions of composite spectra achieved from both IREs were shown in Figure 4.18. To make sure that the absorption magnitudes of spectra are different, the 3D of color code was shown. The observed map revealed the large variation of the absorbance. The large variation of the unique absorption of both polypropylene and hydroxyapatite were greater than that of the noise level. The noise level (peak-to-peak noise) of the observed spectra was 0.02 for Ge μIRE and 0.02 absorbance unit for diamond μIRE. It is indicated that, the variation of absorption intensity of each absorption band is influent from the non-homogeneous distribution of each component.

The 3D profile of absorption band at 2917 $cm^{-1}$ corresponding to the concentration profile of C-H stretching of polypropylene is shown in Figure 4.18 (A2) while the absorption band at 1030 $cm^{-1}$ shows the concentration of P-O stretching of hydroxyapatite is shown in Figure 4.18 (B2). For the characterization using diamond μIRE as seen in the Figure 4.18 (B2), it was found that if the concentration of polypropylene is high (red code), the concentration of hydroxyapatite is low. However, the characterization by using Ge μIRE as seen in the Figure 4.18 (A2) is not in the same direction. The two major reasons were assumed. The first, the surface of specimen is rough in some position. The good contact between the Ge μIRE and rough surface was not achieved. The second, the characterization by using Ge μIRE and diamond μIRE was not constructed in the same area.

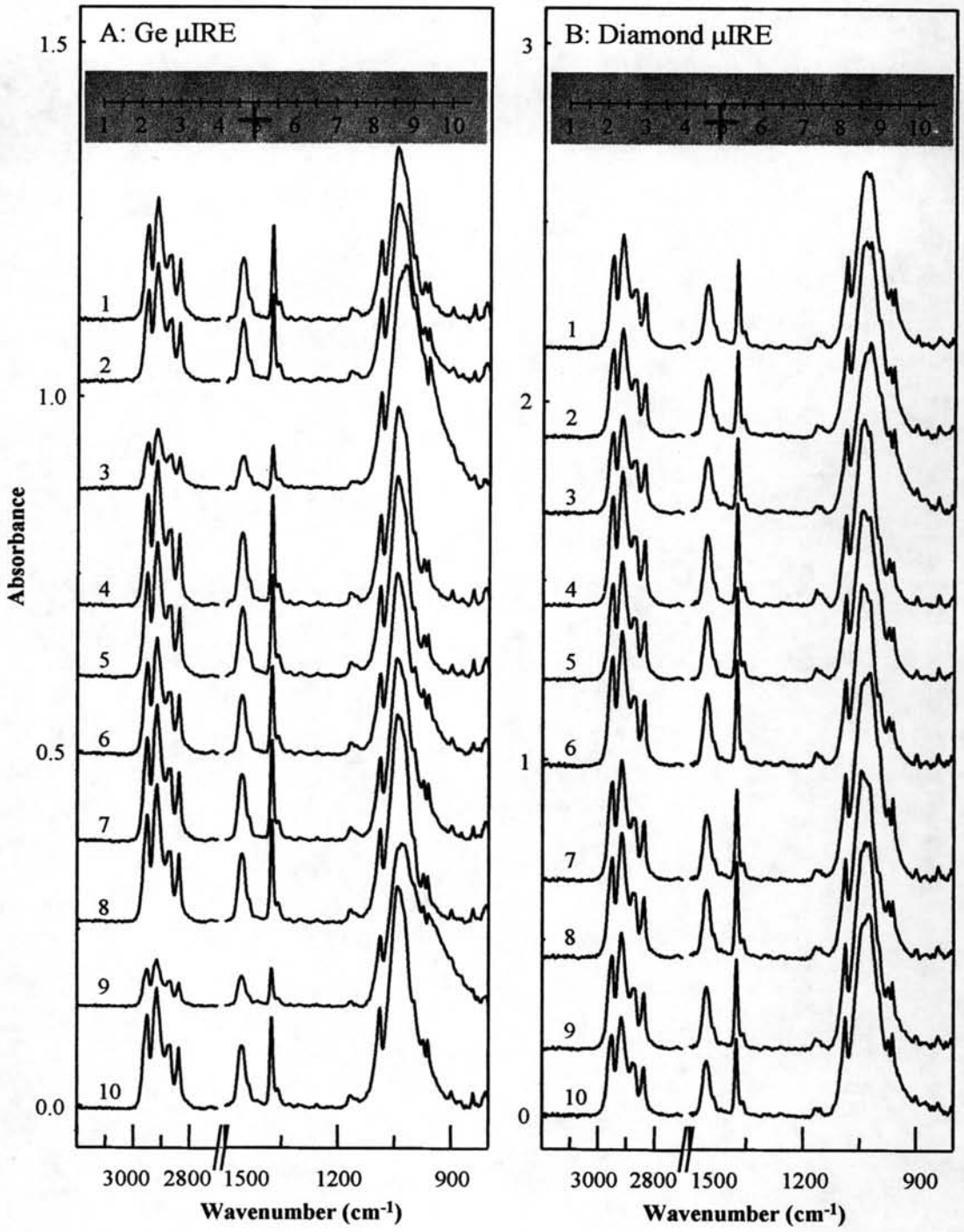


**Figure 4.17** ATR FT-IR spectra at selected position on the cross-section surface of hydroxyapatite/polypropylene composite specimen measured by (A) Ge μIRE and (B) diamond μIRE.

The observed phenomena indicated that hydroxyapatite was not homogeneously distributed with the polypropylene matrix. As the results, the observed phenomena suggested that ATR FT-IR spectra at various positions of non-homogeneous polymer composites were not superimposed while the surface chemical map showed large variation of absorbance.

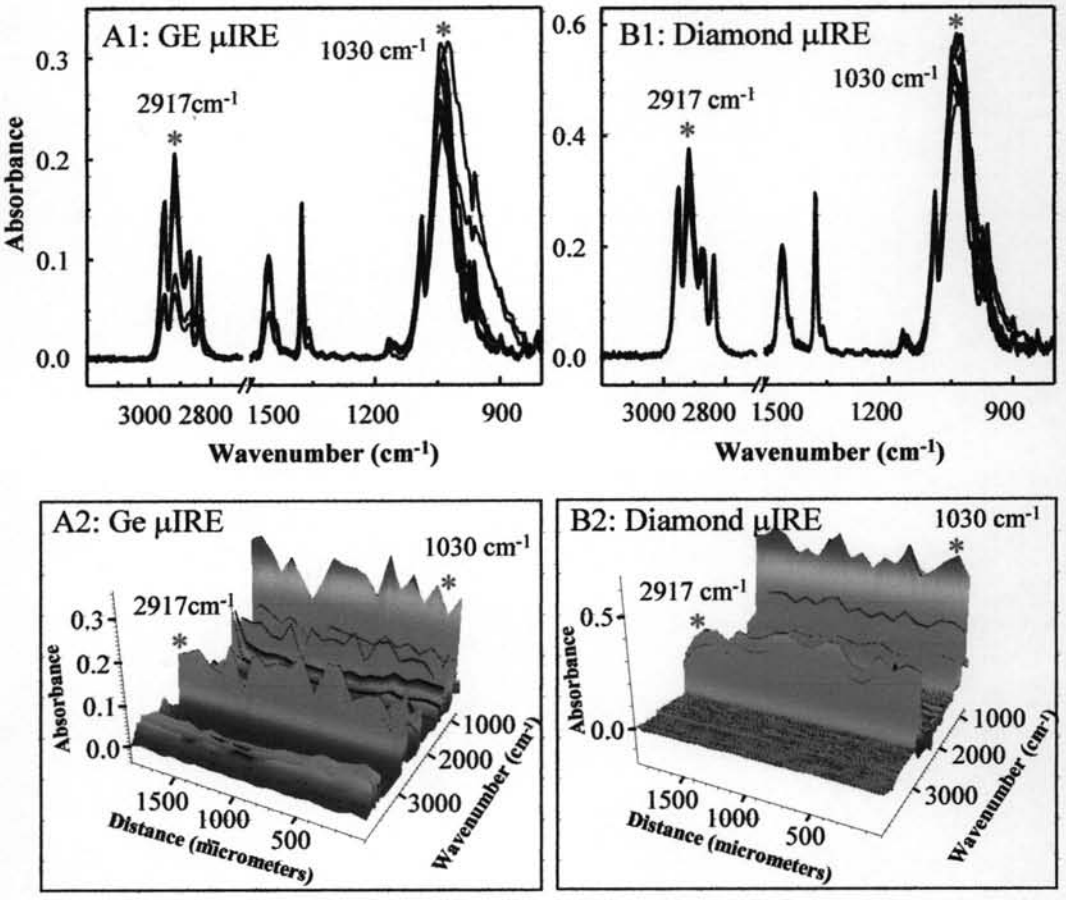


**Figure 4.18** Superimposition of ATR FT-IR spectra of hydroxyapatite/ polypropylene composite were acquired by (A) Ge μIRE and (B) diamond μIRE. Figure A2 and B2 are 3D image of absorption band of the polypropylene/hydroxyapatite composite.

### 4.4.2 Polybenzoxazine and Its Composites

#### 4.4.2.1 Polybenzoxazine

Polybenzoxazine is a new class of thermosetting resins based on bisphenol A and aniline. It can be used as the matrix of high performance composites because of its superior mechanical properties and high temperature stability. The specimen of polybenzoxazine in this study is 6,6′-Bis(3-(3,5-dimethyl)phenyl-3,4-dihydro-2*H*-1,3-benzoxazinyl)isopropane (BA-35x) [8].

The homogeneity characterization of hard and rigid materials like polybenzoxazine (benzoxazine resin) and its composites by area mapping was not investigated. For hard materials, the good contact between IRE and surface of specimen was not achieved. Therefore, the degree of contact between IRE and the specimen cannot be controlled by automatic sensor plate. In this section, the degree of contact in area mapping was manually controlled.

Figure 4.19 (A) shows normalized ATR FT-IR spectra of polybenzoxazine characterized by Ge μIRE. The specimen was characterized without additional sample preparation, accept it was mount onto a glass slide. The spectra acquired by Ge μIRE revealed the same characteristic absorption as that of the resin. It means that, the component of the composites at various positions are the same. The peak assignments of polybenzoxazine are shown in Table 4.4. Figure 4.20 (A) shows the superimposition of ATR FT-IR spectra. The observed phenomena suggested that ATR FT-IR spectra of polybenzoxazine were not superimposed. It was implied that a sufficient contact between the IRE and the surfaces of the solids was not achieved in the experiment with Ge μIRE.

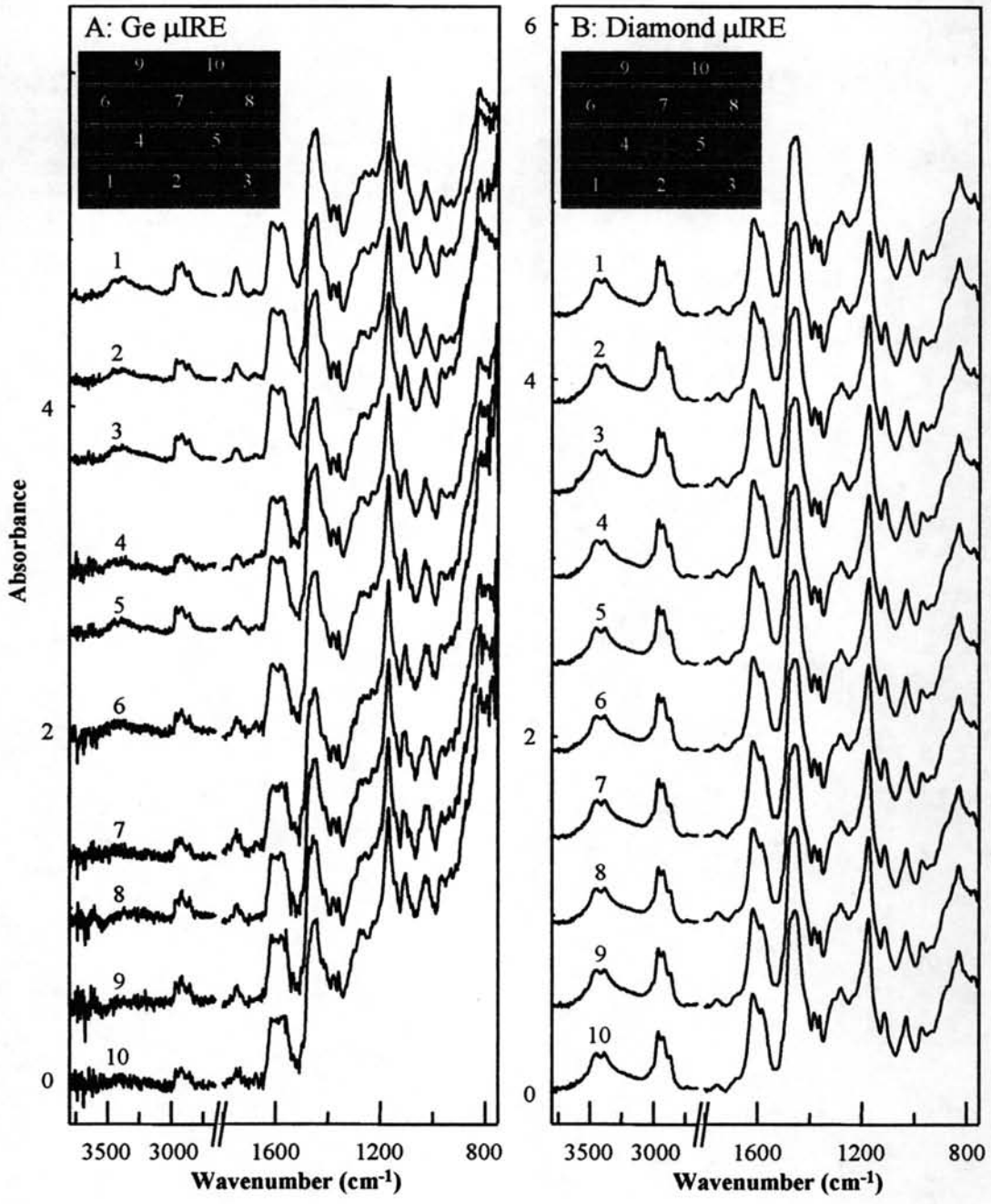


**Figure 4.19** Normalized ATR FT-IR spectra (with absorption at 1458 $cm^{-1}$ as the normalized intensity) at selected position on the surface of polybenzoxazine specimen measured by (A) Ge μIRE and (B) diamond μIRE.

For the characterization of polybenzoxazine with the diamond μIRE, the small culet of the diamond made an unnoticeable dent on the surface of the specimen, as shown in the image in Figure 4.19 (B). As the surface attained an optical contact with the pavilion facet, its ATR FT-IR spectra could be acquired. Normalized ATR FT-IR spectra were shown in Figure 4.19 (B). The spectra acquired by diamond μIRE show the same characteristic absorption as that of the resin. It means that, the component of the composites at various positions are the same. The superimposition of polybenzoxazine spectra are shown in Figure 4.20 (B). The observed phenomena suggested that ATR FT-IR spectra of polybenzoxazine were superimposed at all positions. It is concluded that polybenzoxazine is homogeneous sample.

As the results, it was implied that an insufficient contact between the IRE and the surfaces of the hard and rigid solids was obtained in the experiment with Ge μIRE. Thus, the polybenzoxazine composites can be only analyzed by the diamond μIRE.

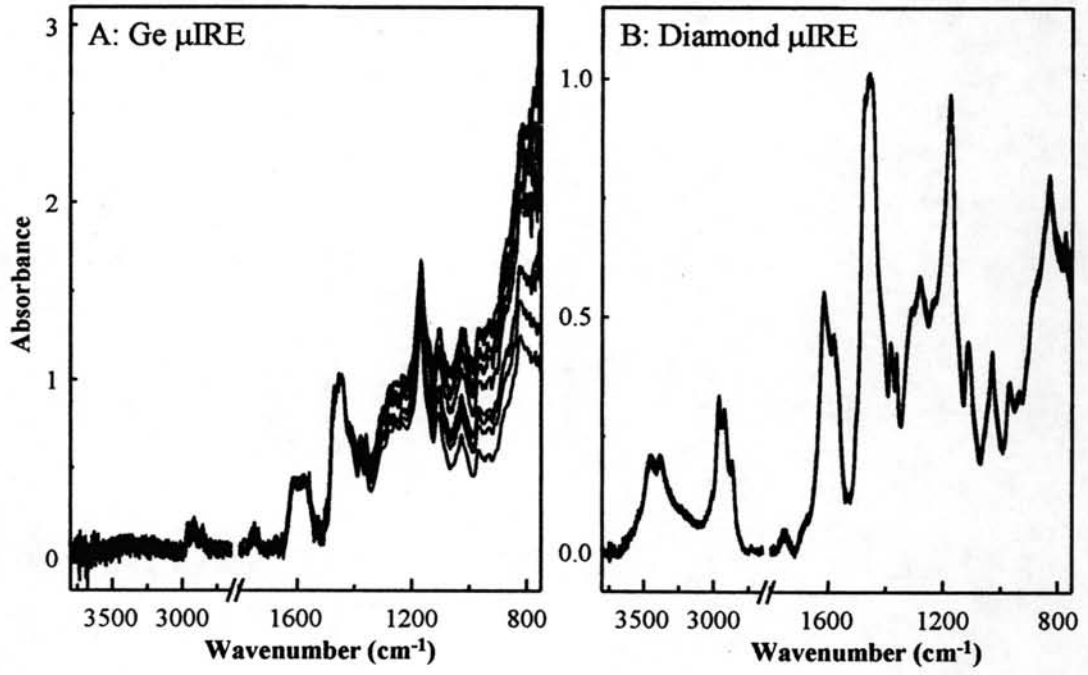


**Figure 4.20** Superimpositions of normalized ATR FT-IR spectra (with absorption at 1458 $cm^{-1}$ as the normalized intensity) of polybenzoxazine were acquired by (A) Ge IRE and (B) diamond IRE.

**Table 4.4** Infrared peak assignments of polybenzoxazine [39].

| Peak Position ($cm^{-1}$) | Assignments |
|---|---|
| 3550-3230 | O-H stretching of phenol |
| 3015 | C-H stretching of aromatic |
| 2961 | Asymmetric C-H stretching of $CH_3$ |
| 2922 | Symmetric C-H stretching of Ar-$CH_3$ |
| 2869 | Symmetric C-H stretching of $CH_3$ |
| 1615, 1581 | C=C stretching of aromatic |
| 1458, 1382 | C-H bending of $CH_3$ |
| 1361 | C-N (-Ar) asymmetric stretching of aliphatic aromatic amine |
| 1280 | C-N stretching of aromatic amine |
| 1173 | C-C stretching in Ar-C(-C)-Ar |
| 1113 | C-N stretching of aliphatic amine |
| 881 | C-H out of plane vibration in term of isolated hydrogen atom of 1,2,3,5-Tetrasubstitued benzenes |
| 828 | C-H out of plane deformation of 1,2,3,5-Tetra-substituted benzenes |

#### 4.4.2.2 Polybenzoxazine/$SiO_2$ (7%) Composite

Polybenzoxazine composite composes of benzoxazine resin and 7% $SiO_2$. The particles of $SiO_2$ in nanometer size were used in composite. The sample was prepared by compression molding technique. Small additional sample preparation was required. The homogeneity characterization by diamond μIRE, the small culet of the diamond made an unnoticeable dent on the surface of the specimen, as shown in Figure 4.21. Figure 4.21 showed the normalized ATR FT-IR spectra of polybenzoxazine/$SiO_2$ (7%) composite. Peak assignments of composites are shown in Table 4.5. The same spectral feature of the resin and filler at various positions were observed. Since the infrared absorption band is unique to the chemical constituent, thus it is clearly seen that the chemical composition of polybenzoxazine/$SiO_2$ (7%) composite at various positions are the same.

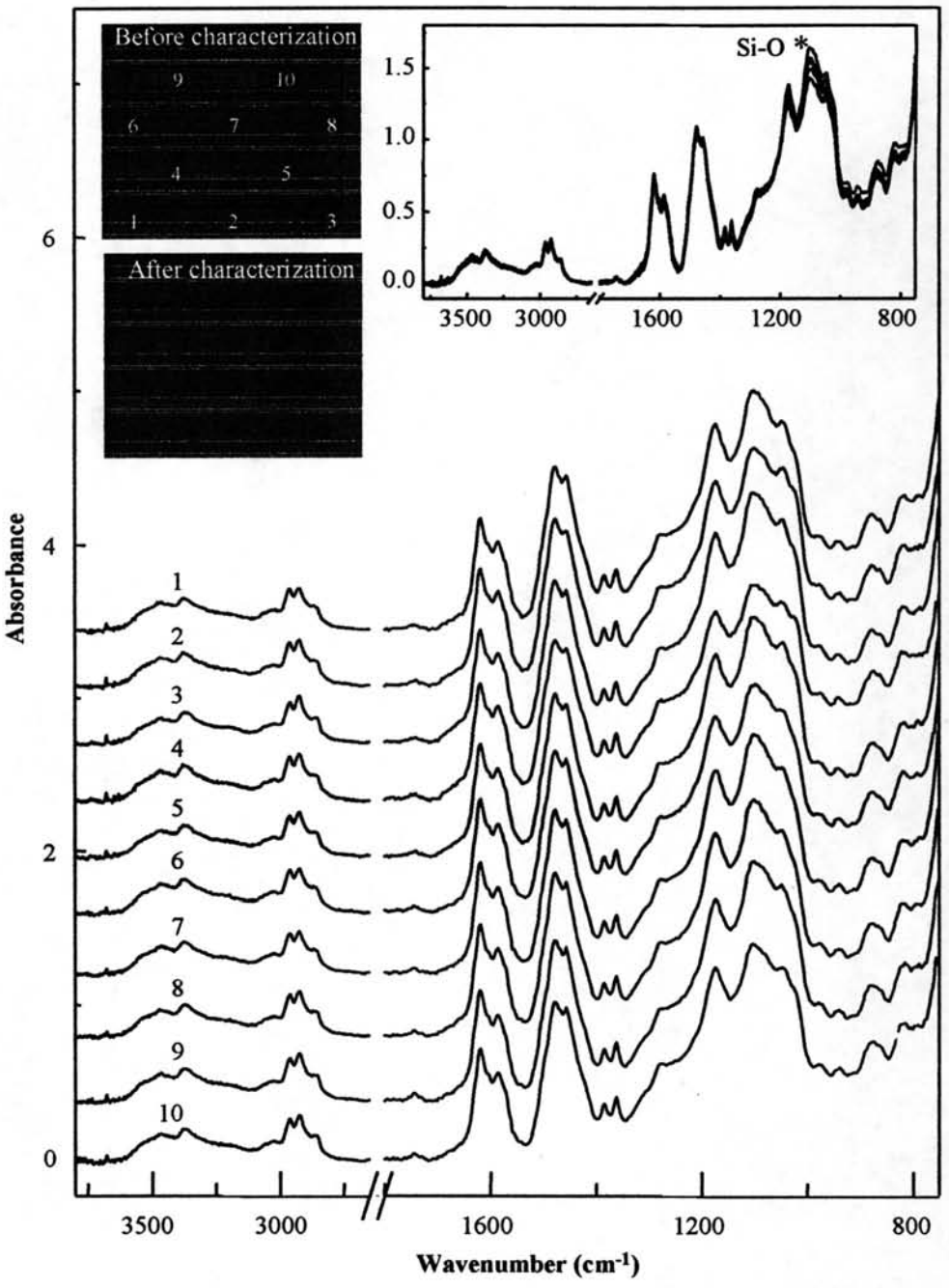


**Figure 4.21** Normalized ATR FT-IR spectra (with absorption at 1458 $cm^{-1}$ as the normalized intensity) at selected position on the surface of polybenzoxazine/$SiO_2$ (7%) composite specimen measured by diamond μIRE.

According to the observed spectra of polybenzoxazine/$SiO_2$ (7%) composite in Figure 4.21, it is clearly seen that the obtained spectra are not superimposed at all characteristic bands, especially the peak position of $SiO_2$ absorption at 1108, 1049, 976 and 942 $cm^{-1}$. The observed spectra revealed large variation of the absorbance (1.637-1.141 absorbance unit). The large variation of the unique absorption bands of polybenzoxazine/$SiO_2$ (7%) composite was greater than the noise level. The noise level (peak-to-peak noise) of the observed spectra was 0.01 absorbance unit. The absorption magnitude of the infrared absorption band is directly related to concentration of sample. Thus, if the ATR spectra of an identical sample are the same absorption intensity of spectra, it reveals that the sample having the same concentration of composition at various positions. In case of polybenzoxazine/$SiO_2$ (7%) composite, it is concluded that, the variation of absorption intensity of $SiO_2$ is influent from the non-homogeneous distribution of $SiO_2$ within the benzoxazine resin.

**Table 4.5** Infrared peak assignments of polybenzoxazine/$SiO_2$ (7%) composite [39].

| Peak Position ($cm^{-1}$) | Assignments |
|---|---|
| 3550-3230 | O-H stretching of phenol |
| 3015 | C-H stretching of aromatic |
| 2963 | Asymmetric C-H stretching of $CH_3$ |
| 2926 | Symmetric C-H stretching of Ar-$CH_3$ |
| 2854 | Symmetric C-H stretching of $CH_3$ |
| 1618, 1585 | C=C stretching of aromatic |
| 1458, 1384 | C-H bending of $CH_3$ |
| 1361 | C-N (-Ar) asymmetric stretching of aliphatic aromatic amine |
| 1284 | C-N stretching of aromatic amine |
| 1173 | C-C stretching in Ar-C(-C)-Ar |
| 1108, 1049 | Asymmetric. Si-O-C stretching |
| 976, 942 | Symmetric Si-O-C stretching |
| 878 | C-H out of plane vibration in term of isolated hydrogen atom of 1,2,3,5-Tetrasubstitued benzenes |
| 819 | C-H out of plane deformation of 1,2,3,5-Tetra-substituted benzenes |

#### 4.4.2.3 Polybenzoxazine/$Al_2O_3$ (40%) Composite

Polybenzoxazine composite was prepared by compression molding technique. The composite composes of benzoxazine resin and 40% $Al_2O_3$. The micrometric particles of $Al_2O_3$ were used in composite. For the analysis, the small additional sample preparation was required. The homogeneity characterization by diamond μIRE, the small culet of the diamond made an unnoticeable dent on the surface of the specimen, as shown the image in Figure 4.22. Thus the problem associated with the contact between the sample surface and tip of diamond was not observed.

Figure 4.22 showed normalized ATR FT-IR spectra of polybenzoxazine/$Al_2O_3$ (40%) composite acquired by the diamond μIRE. The peak assignments of those composites are shown in Table 4.6. The absorption character of the resin and filler were observed. All ATR FT-IR spectra showed the same absorption feature. It is indicated that, the components of composite are the same at various positions on the surface of specimen. The superimposition of polybenzoxazine/$Al_2O_3$ (40%) composite was shown in Figure 4.22. Although, the absorption band of $Al_2O_3$ is not clear, the observed phenomena suggested that ATR FT-IR spectra of composites were superimposed for all positions. The obtained spectra revealed the small variation of the absorbance, this variation is comparable to the noise level. The noise level of the observed spectra was 0.02 absorbance unit.

Figure 4.22 shows the ATR FT-IR spectrum of polybenzoxazine/$Al_2O_3$ (40%) composite at the absorption band of $Al_2O_3$ is not clear when comparison with the spectrum acquires by the specular reflection technique (Figure 4.4 (D)). Due to the different of sampling technique, such as specular reflection, transmission, and attenuated total reflection, the produce spectra that differ in frequency, shape, and intensity of band though the sample is the same [33]. For specular reflection technique, the spectrum can easily to interpret when Kramers-Kronig (KK) transformation is employed for making a specular reflection spectrum becoming absorption-like spectrum. The mathematic equation is directly concerned with the refractive index, $n$, and absorption index, $k$ (equation 2.7). Since the refractive index, $n$, and absorption index, $k$, determine the response of a material to incident

electromagnetic radiation, or referred as the optical constant (Chapter II). However, they do not strictly constant because they vary with frequency. Then, the absorption band of $Al_2O_3$ acquired by specular reflection technique is clear because the KK-transformation making the absorption band of $Al_2O_3$ shift to high wavenumber.

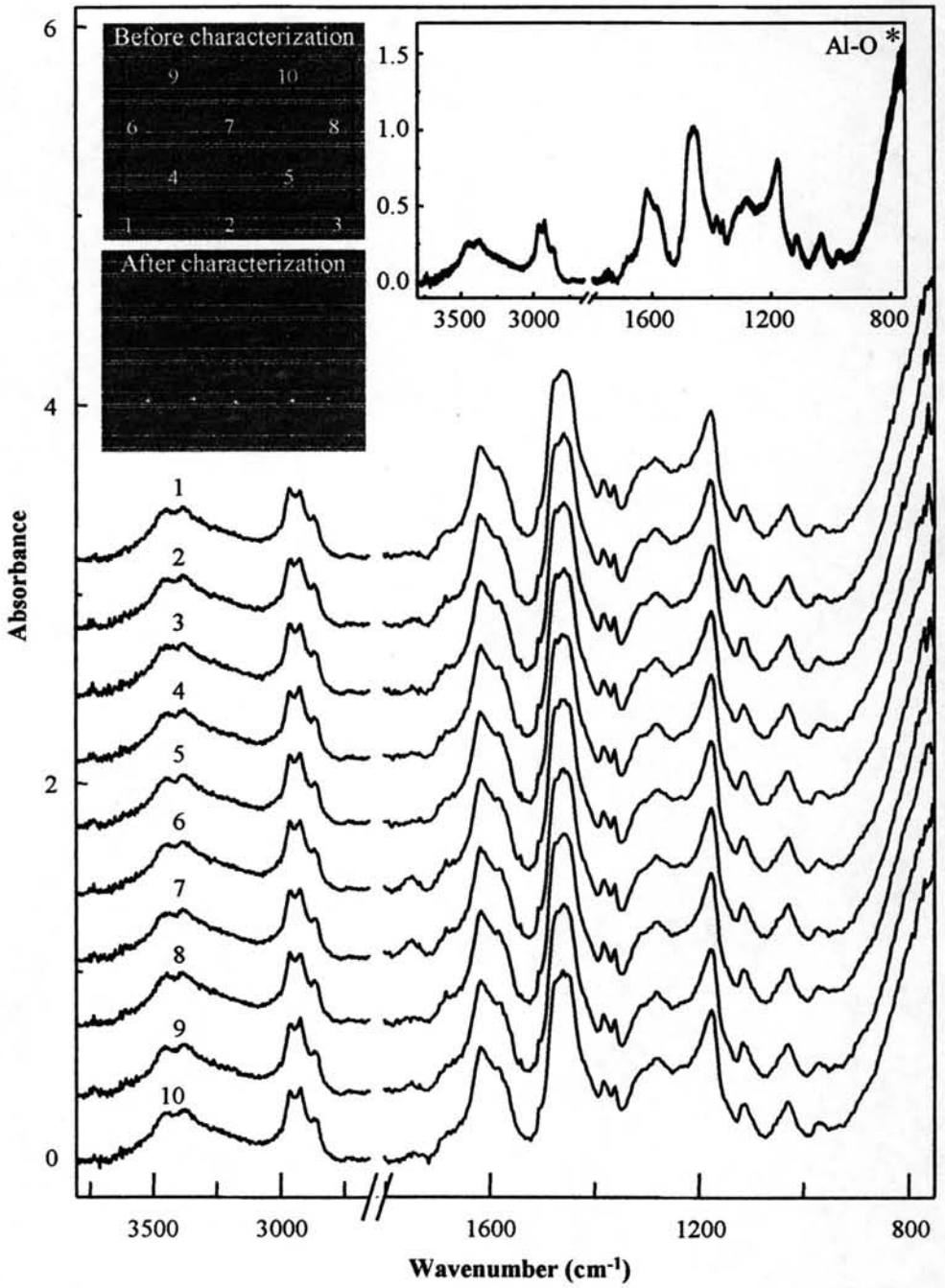


**Figure 4.22** Normalized ATR FT-IR spectra (with absorption at 1458 $cm^{-1}$ as the normalized intensity) at selected position on the surface of polybenzoxazine/$Al_2O_3$ (40%) composite specimen measured by diamond μIRE.

As the results, although the absorption bands of $Al_2O_3$ are not clear, it is concluded that $Al_2O_3$ has the same concentration at various points on the surface of the specimen. On the other hand, $Al_2O_3$ is homogeneously distributed within the benzoxazine resin at all positions.

**Table 4.6** Infrared peak assignments of polybenzoxazine/$Al_2O_3$ (40%) composite [39].

| Peak Position ($cm^{-1}$) | Assignments |
|---|---|
| 3550-3230 | O-H stretching of phenol |
| 3015 | C-H stretching of aromatic |
| 2960 | Asymmetric C-H stretching of $CH_3$ |
| 2925 | Symmetric C-H stretching of Ar-$CH_3$ |
| 2866 | Symmetric C-H stretching of $CH_3$ |
| 1616, 1580 | C=C stretching of aromatic |
| 1458, 1382 | C-H bending of $CH_3$ |
| 1362 | C-N (-Ar) asymmetric stretching of aliphatic aromatic amine |
| 1282 | C-N stretching of aromatic amine |
| 1173 | C-C stretching in Ar-C(-C)-Ar |
| 878 | C-H out of plane vibration in term of isolated hydrogen atom of 1,2,3,5-Tetrasubstitued benzenes |
| 827 | C-H out of plane deformation of 1,2,3,5-Tetra-substituted benzenes |
| 860-750 | Al-O stretching |

#### 4.4.2.4 Polybenzoxazine/$SiC_{(particle)}$ (10%) Composite

For the characterization of the homogeneity of polybenzoxazine/$SiC_{(particle)}$ (10%) composite, the sample was prepared by compression molding technique. Polybenzoxazine composite composes of benzoxazine resin and 10% $SiC_{(particle)}$. The particle of SiC in micrometric size was used in composite. The small culet of the diamond made an unnoticeable dent on the surface of the specimen, the image shown in Figure 4.23. As the surface attained an optical contact with the pavilion facet, its ATR FT-IR spectra could be acquired. Figure 4.23 showed normalized ATR FT-IR

spectra of polybenzoxazine/$SiC_{(particle)}$ (10%) composite. The characteristic absorptions of the resin and filler were observed. All ATR FT-IR spectra, showed the same absorption feature. It is indicated that, the components of composite are the same at various positions on the near surface of specimen. The peak assignments of composite are shown in Table 4.7.

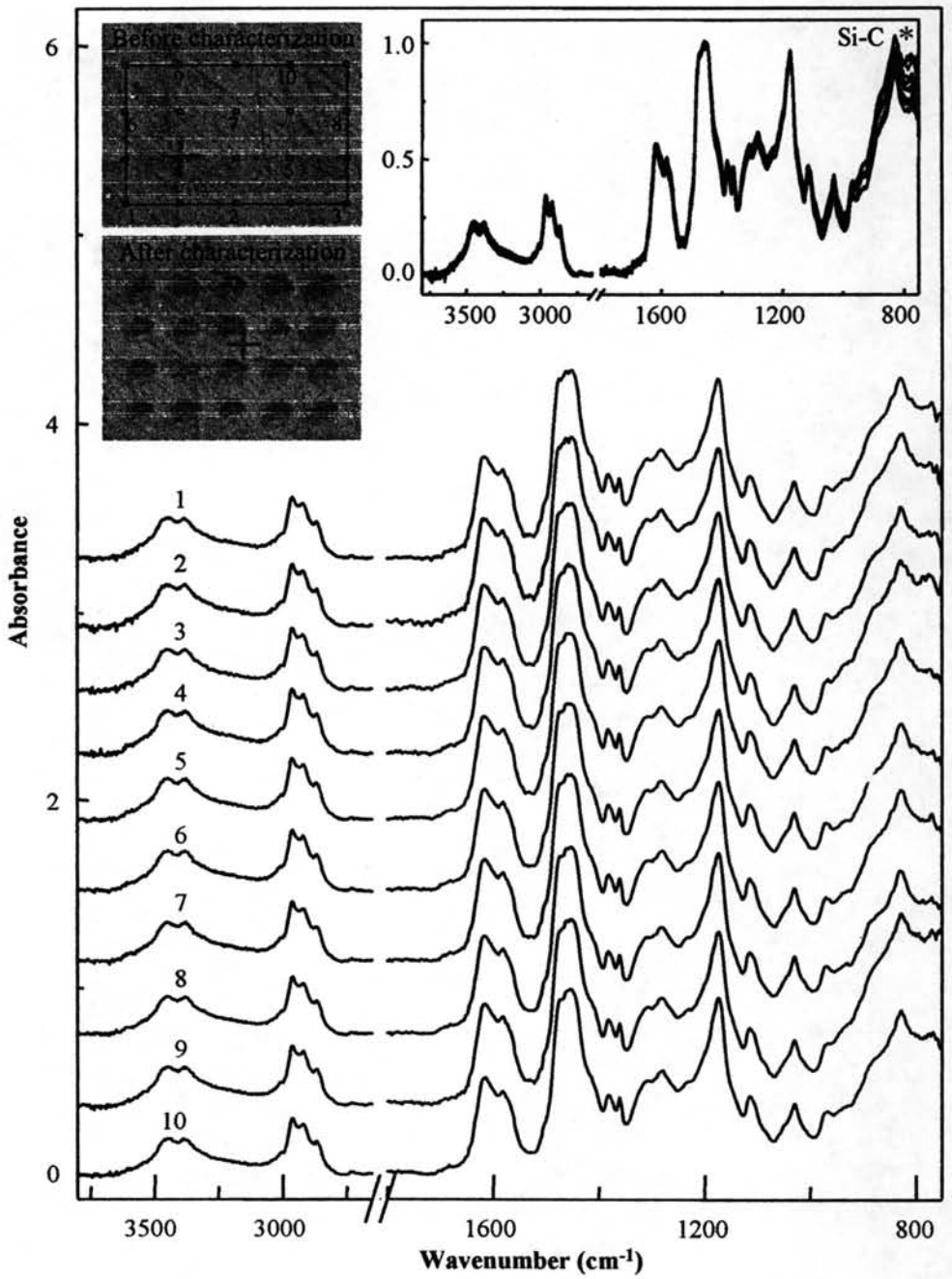


**Figure 4.23** Normalized ATR FT-IR spectra (with absorption at 1458 $cm^{-1}$ as the normalized intensity) at selected position on the surface of polybenzoxazine/$SiC_{(particle)}$ (10%) composite specimen measured by diamond μIRE.

According to the observed spectra of polybenzoxazine/$SiC_{(particle)}$ (10%) composite in Figure 4.23, it is clearly seen that the obtained spectra are not superimposed, especially the peak position of SiC absorption at 780-800 $cm^{-1}$. Although, the absorption band of SiC is not clear, the obtained spectra revealed largely in the variation of the absorbance at 850-750 $cm^{-1}$. This variation is greater than the noise level. The noise level (peak-to-peak noise) of the observed spectra was 0.02 absorbance unit. Since the absorption intensity of ATR spectra is related to the concentration of composition of composite, thus the variation of absorption intensity at region of SiC is influent from the difference of the concentration of composition, or the non-uniform distribution of SiC through the benzoxazine resin.

**Table 4.7** Infrared peak assignments of polybenzoxazine/$SiC_{(particle)}$ (10%) composite [39].

| Peak Position ($cm^{-1}$) | Assignments |
|---|---|
| 3550-3230 | O-H stretching of phenol |
| 3015 | C-H stretching of aromatic |
| 2960 | Asymmetric C-H stretching of $CH_3$ |
| 2919 | Symmetric C-H stretching of Ar-$CH_3$ |
| 2867 | Symmetric C-H stretching of $CH_3$ |
| 1614, 1581 | C=C stretching of aromatic |
| 1458, 1381 | C-H bending of $CH_3$ |
| 1361 | C-N (-Ar) asymmetric stretching of aliphatic aromatic amine |
| 1279 | C-N stretching of aromatic amine |
| 1173 | C-C stretching in Ar-C(-C)-Ar |
| 878 | C-H out of plane vibration in term of isolated hydrogen atom of 1,2,3,5-Tetrasubstitued benzenes |
| 827 | C-H out of plane deformation of 1,2,3,5-Tetra-substituted benzenes |
| 800 | Si-C stretching |

### 4.4.2.5 Polybenzoxazine/$SiC_{(wisker)}$ (10%) Composite

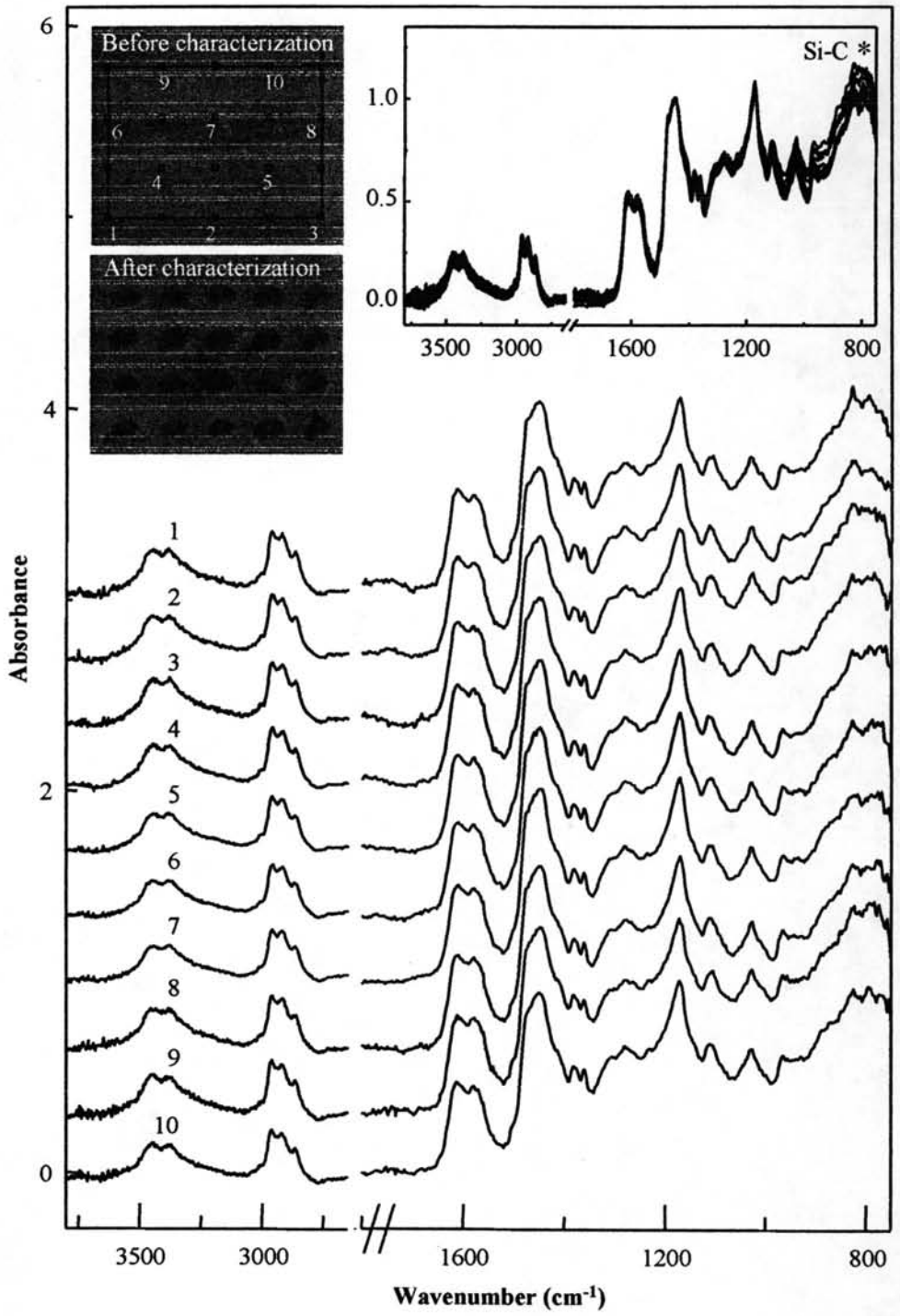


**Figure 4.24** Normalized ATR FT-IR spectra (with absorption at 1458 $cm^{-1}$ as the normalized intensity) at selected position on the surface of polybenzoxazine/$SiC_{(wisker)}$ (10%) composite specimen measured by diamond μIRE.

Polybenzoxazine composite composes of benzoxazine resin and 10% $SiC_{(wisker)}$. The $SiC_{(wisker)}$ in micrometric size was used in composite. The sample was prepared by compression molding technique and no additional sample preparation. The homogeneity characterization by diamond μIRE, the small culet of the diamond made an unnoticeable dent on the surface of the specimen, as shown the image in Figure 4.24. Figure 4.24 showed normalized ATR FT-IR spectra of polybenzoxazine/ $SiC_{(wisker)}$ (10%) composite. The same spectral feature of the resin and filler at various positions were observed. Since the unique infrared absorption band is related to the chemical compositions of sample, the same chemical information of spectra reveal that the compositions of composite are the same.

**Table 4.8** Infrared peak assignments of polybenzoxazine/$SiC_{(wisker)}$ (10%) composite [39].

| **Peak Position ($cm^{-1}$)** | **Assignments** |
|---|---|
| 3550-3230 | O-H stretching of phenol |
| 3015 | C-H stretching of aromatic |
| 2960 | Asymmetric C-H stretching of $CH_3$ |
| 2917 | Symmetric C-H stretching of Ar-$CH_3$ |
| 2859 | Symmetric C-H stretching of $CH_3$ |
| 1611, 1578 | C=C stretching of aromatic |
| 1458, 1381 | C-H bending of $CH_3$ |
| 1361 | C-N (-Ar) asymmetric stretching of aliphatic aromatic |
| 1278 | C-N stretching of aromatic amine |
| 1172 | C-C stretching in Ar-C(-C)-Ar |
| 878 | C-H out of plane vibration in term of isolated hydrogen atom of 1,2,3,5-Tetrasubstitued benzenes |
| 824 | C-H out of plane deformation of 1,2,3,5-Tetra-substituted benzenes |
| 800 | Si-C stretching |

Peak assignments of composite are shown in Table 4.8. According to the observed spectra of polybenzoxazine/$SiC_{(wisker)}$ (10%) composite in Figure 4.24, it is clearly seen that the obtained spectra are not superimposed at all characteristic bands, especially the peak position of SiC absorption at 780-800 $cm^{-1}$. The observed spectra revealed largely in variation of the absorbance. The large variation of the unique absorption bands of polybenzoxazine/$SiC_{(wisker)}$ (10%) composite was greater than the noise level. The noise level (peak-to-peak noise) of the observed spectra was 0.02 absorbance unit. Since the absorption intensity of the absorption band is directly related to concentration of sample, the non-equivalent of absorption intensity of and identical sample in ATR spectra reveal that $SiC_{(wisker)}$ is non-uniform distribution through the benzoxazine resin. On other hand, the polybenzoxazine/$SiC_{(wisker)}$ (10%) composite is non-homogeneous sample.